Contrib Mineral Petrol (1991) 106:183–200

Contributions to Mineralogy and Petrology

The tholeiite to alkalic basalt transition at Haleakala Volcano, Maui, Hawaii

C.-Y. Chen[1], F.A. Frey[2], M.O. Garcia[3], G.B. Dalrymple[4], and S.R. Hart[5]

[1] Department of Geology, University of Illinois, Urbana, IL 61801, USA
[2] Department of Earth, Atmospheric, and Planetary Sciences, MIT, Cambridge, MA 02139, USA
[3] Department of Geology and Geophysics, University of Hawaii, Honolulu, HI 96822 USA
[4] U.S. Geological Survey, Menlo Park, CA 94025, USA
[5] Woods Hole Oceanographic Institution, Woods Hole, MA 02543, USA

Received April 4, 1990 / Accepted July 17, 1990

Abstract. Previous studies of alkalic lavas erupted during the waning growth stages (<0.9 Ma to present) of Haleakala volcano identified systematic temporal changes in isotopic and incompatible element abundance ratios. These geochemical trends reflect a mantle mixing process with a systematic change in the proportions of mixing components. We studied lavas from a 250-m-thick stratigraphic sequence in Honomanu Gulch that includes the oldest (~1.1 Ma) subaerial basalts exposed at Haleakaka. The lower 200 m of section is intercalated tholeiitic and alkalic basalt with similar isotopic (Sr, Nd, Pb) and incompatible element abundance ratios (e.g., Nb/La, La/Ce, La/Sr, Hf/Sm, Ti/Eu). These lava compositions are consistent with derivation of alkalic and tholeiitic basalt by partial melting of a compositionally homogeneous, clinopyroxene-rich, garnet lherzolite source. The intercalated tholeiitic and alkalic Honomanu lavas may reflect a process which tapped melts generated in different portions of a rising plume, and we infer that the tholeiitic lavas reflect a melting range of ~10% to 15%, while the intercalated alkalic lavas reflect a range of ~6.5% to 8% melting. However, within the uppermost 50 m of section, $^{87}Sr/^{86}Sr$ decreases from 0.70371 to 0.70328 as eruption age decreased from ~0.97 Ma to 0.78 Ma. We infer that as lava compositions changed from intercalated tholeiitic and alkalic lavas to only alkalic lavas at ~0.93 Ma, the mixing proportions of source components changed with a MORB-related mantle component becoming increasingly important as eruption age decreased.

Introduction

During the transition from the shield-building tholeiitic stage to the postshield stage, eruption rates at Hawaiian volcanoes decrease (Feigenson and Spera 1981; Frey et al. 1990), and both tholeiitic and alkalic basalts are erupted (Table 1.1 Clague and Dalrymple 1987). In order to understand the processes of magma generation and evolution at Hawaiian volcanoes, it is important to define and interpret temporal geochemical changes during the transition from tholeiitic to alkalic volcanism. Previous studies showed that the postshield alkalic lavas at Haleakala Volcano define systematic temporal trends in $^{87}Sr/^{86}Sr$ and $^{143}Nd/^{144}Nd$ isotopic ratios, and abundance ratios of highly incompatible elements, such as La/Ce (Chen and Frey 1985; West and Leeman 1987; Chen et al. 1990). These geochemical trends have been related to mixing of melts derived from a mantle plume source and a depleted, MORB-related lithosphere, with the tholeiitic lavas containing the largest proportion of the plume component (Chen and Frey 1985). However, tholeiitic lavas from Haleakala and the transition from tholeiitic to alkalic volcanism at Haleakala have not been studied in detail. We studied the oldest subaerial lavas exposed on Haleakala – a section of interbedded tholeiitic and alkalic lavas. Our results show that lavas (12 tholeiitic and 5 alkalic) from the lower 200 m of section have similar isotopic ratios (Sr, Nd and Pb) and abundance ratios of elements with similar incompatibility (e.g., Nb/La, La/Ce, P/Nd, and Hf/Sm). We conclude that these lavas resulted from varying degrees of melting of a compositionally homogeneous source. In contrast, within the upper 50 m of section there is an upsection decrease in $^{87}Sr/^{86}Sr$ ratios. This temporal variation in $^{87}Sr/^{86}Sr$ correlates with the systematic temporal trend found previously in younger Haleakala lavas (Chen and Frey 1983, 1985; West and Leeman 1987).

Regional geology of Haleakala

Haleakala last erupted in 1790; therefore, it is an active volcano (Macdonald et al. 1983). Volcanic activity has been concentrated in the summit area and along the southwest, east and more poorly developed north rift zones (Fig. 1). Erosion has deeply dissected the windward (east) side of Haleakala exposing 100 to 250 m thick

Offprint requests to: C.-Y. Chen

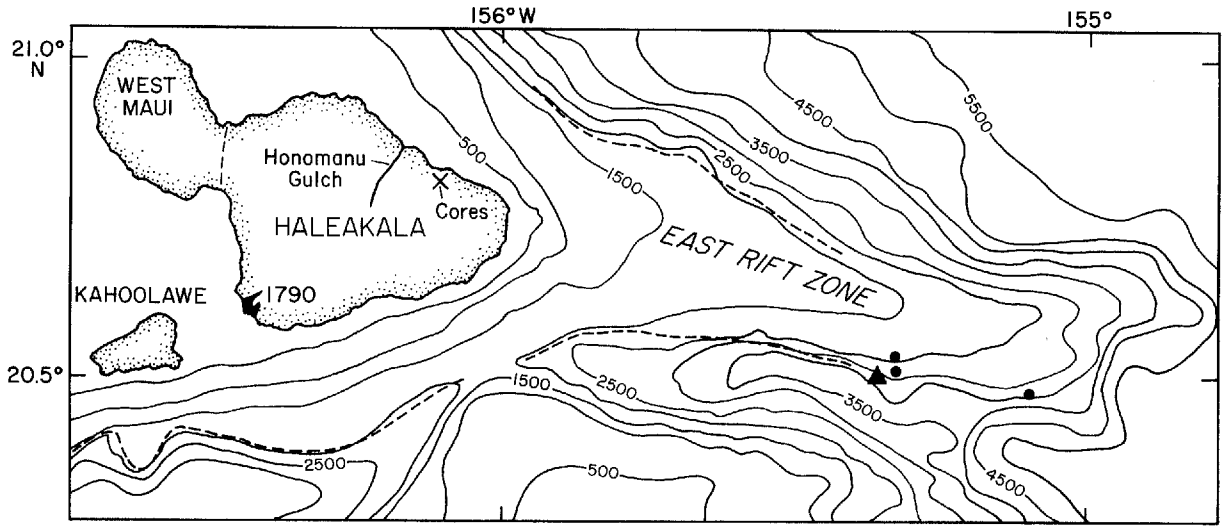

Fig. 1. Location map for the Haleakala samples discussed in the text. The Honomanu Gulch and Nahiku core samples were collected from the northeast side of the volcano, which is subject to high rainfall and is deeply dissected. The 1790 flow is the most recent eruption of Haleakala and is located along its southwest rift zone. The submarine samples were dredged from the east rift zone of Haleakala which extends for about 135 km offshore (bathymetry from Wilde et al. 1980). The *triangle* shows the location of our dredge haul; *closed circles* show location of dredges by Moore et al. (1990) that recovered volcanic glass. *Dashed line* indicates approximate location of the major slope break which is thought to mark the shoreline of Haleakala at the end of the shield-building stage (Moore and Campbell 1987)

sections. (Stearns and Macdonald (1942) subdivided the volcanic rocks into three units, now named: the Honomanu Basalt (shield), the Kula Volcanics (alkalic cap or postshield), and the Hana Volcanics (post-erosional) (Langenheim and Clague 1987). A soil horizon separates each formation although thinner soils are present within formations. Locally, an erosional surface with up to 1 km of relief separates the Kula and Hana lavas. A slope break that is thought to mark sea level during active shield development is now 1.5 to 2.5 km below sea level (Moore and Campbell 1987; Moore et al. 1990). Moore and Fiske (1969) proposed that when this slope break subsides below sea level it marks the end of shield volcanism. The age of this slope has been estimated at 0.85 Ma (Moore and Campbell 1987), and a coral reef sampled 300 m above the slope break has been dated as 750 ± 13 ka (Moore et al. 1990). Because dredging above the slope break recovered tholeiitic basalt, Moore et al. (1990) concluded that a transition from tholeiitic to alkalic volcanism did not coincide with the end of voluminous shield building.

The oldest subaerial Haleakala lavas are in Honomanu Gulch (Stearns and Macdonald 1942). We collected samples from this gulch in order to supplement the reconnaissance sampling by Macdonald and Katsura (1964). These samples are from a composite section of ~250 m (Fig. 2). Recent geochemical studies of Haleakala lavas have focused on the thick sections (~300 m) of Kula and Hana lavas from drill cores taken ~15 km southeast of the Honomanu Gulch (Chen and Frey 1985; Chen et al. 1990) and outcrops from the summit area (West and Leeman 1987). The Kula section in the Honomanu Gulch is only about 20 m thick but the gulch exposes over 230 m of Honomanu lavas (Fig. 2). This paper focuses on the geochemical variations within Honomanu lavas and compares these lavas to the well characterized younger Kula lavas which are all alkalic, and a suite of submarine glasses dredged from the east rift of Haleakala (Moore et al. 1990) (Fig. 1).

Analytical techniques

Nineteen samples from a stratigraphic section of the Honomanu Basalt (Fig. 2) were analyzed for major element, H_2O^+, CO_2, trace element (Sc, V, Cr, Co, Ni, Zn, Rb, Sr, Ba, rare earth element, Hf, Ta, and Th) abundances (Table 1). Three Kula samples which directly overlie these Honomanu lavas (Fig. 2), a Hana lava from the most recent, ~1790, eruption of Haleakala volcano, and a dredged sample from the east rift zone were also analyzed (Table 1). Accuracy and precision of the major and trace element data can be evaluated from replicate analyses of standard rock, BHVO-1 (Table 1).

Representative samples were analyzed for Sr, Nd and Pb isotopic ratios at MIT (Table 1). The 2 sigma analytical uncertainty for Sr and Nd isotopic ratios is less than 0.005%. The 2 sigma analytical uncertainty for Pb isotopes is estimated to be better than 0.05% per mass unit (i.e., $\pm 0.1\%$ for $^{206}Pb/^{204}Pb$, $\pm 0.15\%$ for $^{207}Pb/^{204}Pb$, and $\pm 0.2\%$ for $^{208}Pb/^{204}Pb$).

Three of four samples selected for whole-rock K-Ar dating were free of interstitial glass and visible alteration, and have normal (>1.45) K_2O/P_2O_5 ratios. Sample HO-9 contains minor clays after olivine, but because the alteration does not involve a K-bearing mineral it should not adversely affect the K–Ar age. The samples were crushed to a size of 0.5–1.0 mm. One aliquant of this material was pulverized to a fine powder and used for K_2O analyses, the remaining material was split for the Ar analyses. Argon and K_2O analyses were by isotope dilution and flame photometry, respectively, using methods previously described (Dalrymple and Lanphere 1969; Ingamells 1970). Argon mass analyses were done with a 6-inch, 120° sector, Nier-type mass spectrometer and a 9-inch, 90° sector, multiple collector mass spectrometer (Stacey et al. 1981).

Results

K–Ar ages and paleomagnetic polarities

The age of the Honomanu Basalt was poorly known prior to this study because only one sample had been dated (0.83 ± 0.17 Ma, Naughton et al. 1980). This sample was chosen to represent the oldest exposed Honomanu lavas and was collected in Honomanu Gulch; it came from approximately the same stratigraphic level as C122 (Fig. 2). McDougall (1964) analyzed a Kula lava (the same flow as sample HO-10, Fig. 2) from the

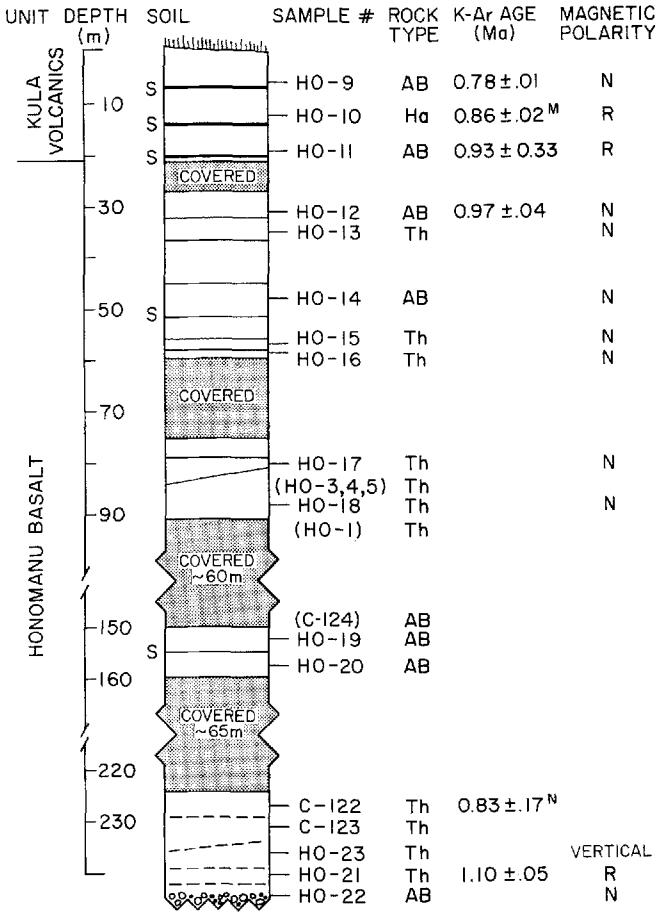

Fig. 2. Composite column section for Honomanu Gulch. Samples HO-9 to HO-20 were collected along the road on the west side of the gulch where the section was measured. Samples HO-1, -3, -4, and -5 were collected along the coast and their stratigraphic positions were projected onto the section using the dip of the section. Samples HO-21 to -23 and C122 and C123 were collected upstream from the road in the gulch. Their relative positions were projected onto the section using the dip of the lavas. The rock types of the samples are: Th – tholeiite; AB – alkalic basalt; and Ha – hawaiite. The K–Ar ages are for new samples (Table 2) and previously reported samples that were collected in the gulch (M – McDougall 1964; N – Naughton et al. 1980). Soil horizons are marked by an S next to their location in the section. The soils within and at the base of the Kula Volcanics are thicker than the soils within the Honomanu Basalt section (5–10 cm vs 1–3 cm). Note the breaks in the section for the two lower covered intervals. The magnetic polarity direction (N = normal, R = reversed) are based on fluxgate magnetometer measurements

upper part of the Honomanu Gulch section and reported an age of 0.86 ± 0.02 Ma (corrected to 1976 IUGS constants).

We dated four new samples from the Honomanu Gulch section. Two are from the lower (HO-21) and uppermost (HO-12) parts of the Honomanu Basalt exposed in Honomanu Gulch. The lowermost Kula lava (HO-11) was also dated to help constrain the end of Honomanu volcanism. The uppermost Kula lava in the section (HO-9) was dated because a well-developed soil horizon separates it from underlying Kula lavas.

The K-Ar analytical data and the resulting calculated ages are shown in Table 2 and Fig. 2. The reproducibility of the Ar analyses for three of the four rocks is less than expected from analytical error. Poor reproducibility has been noted in studies of other Hawaiian rocks (Doell and Dalrymple 1973) and may be due to inhomogeneities, to incipient alteration not detectable in thin section, to unrecognized xenocrystic inclusions that contain inherited ^{40}Ar, or a combination of these causes. As there is no basis for deciding a priori which of these individual measurements are the most representative of the radiogenic ^{40}Ar content of an individual sample, we used the weighted mean of all measurements on a sample as the best age for the sample. Weighting by the inverse of the variance provides a way of combining data of variable quality without the poorer data affecting the results disproportionately (Taylor 1982).

The oldest exposed lavas of the Honomanu Basalt yielded a weighted mean age of 1.10 ± 0.05 Ma, the youngest an age of 0.97 ± 0.04 Ma. Our two samples from the overlying Kula Volcanics have weighted mean ages of 0.93 ± 0.33 Ma (HO-11) and 0.78 ± 0.01 Ma (HO-9). The weighted mean ages of the four samples are consistent with the known stratigraphy and indicate that the lavas in the Honomanu Gulch section accumulated within about 0.4 m.y. or less (Fig. 2). The ages for the two Honomanu samples, which are separated by about 210 m of section, are just statistically different at the 95% level of confidence and are consistent with the high eruption rate of Hawaiian volcanoes (Lockwood and Lipman 1987). The youngest Honomanu and the oldest Kula lavas in the Honomanu Gulch section have very similar K-Ar ages which constrain the end of the Honomanu volcanism to between 0.93 ± 0.33 Ma and 0.97 ± 0.04 Ma. This transition from interbedded tholeiitic and alkalic basalt (Honomanu Basalt) to only alkalic lavas (Kula Volcanics) is older than the estimated age, 0.85 Ma, of the submarine slope break which is interpreted as the morphologic end of shield building (Moore et al. 1990). Because the transition from thin-bedded, porphyritic Honomanu lavas to massive, thick, aphyric Kula lavas is clear in the field, the slope break and the end of tholeiitic volcanism may be older than 0.85 Ma.

The weighted mean age for sample HO-11 (0.93 Ma) is the oldest reported for the Kula Volcanics. The youngest sample in the gulch section (0.78 ± 0.01 Ma) has a weighted mean age within the range reported for the Kula Volcanics (0.4–0.9 Ma; McDougall 1964; Naughton et al. 1980). Thus only flows from the early phase of Kula volcanism reached Honomanu Gulch and they are separated by hiatuses of 60–90 ka. This is consistent with a lower eruption rate during this stage of evolution of Hawaiian volcano (Spengler and Garcia 1988) and the distance of the gulch from the main centers of Kula volcanism.

Fluxgate magnetometer measurements were made on samples from Honomanu Gulch to complement the K–Ar ages. The dated samples yielded unambiguous polarity directions (Fig. 2). With one possible exception, they are consistent with the geomagnetic polarity time scale (Berggren et al. 1985). The oldest sample (HO-21) is reversely magnetized, which is consistent with its age with-

Table 1. Major and trace element abundances and isotopic ratios of the Haleakala lavas and the standard rock, BHVO-1

Sample	BHVO-1	KK83-0725	Honomanu[a]									
			HO-22	HO-21	HO-23	C123	C122	HO-20	HO-19	C124	HO-1	HO-18
Rock type[b]	TH	TH	AB	TH	TH	TH	TH	AB	AB	AB	TH	TH
Depth	–	Dredge	244	240	236	231	227	157	152	140	95	89
SiO_2	49.57±0.49	45.78	46.96	51.23	47.10	45.67	48.05	46.22	47.04	46.61	46.47	46.75
Al_2O_3	13.66±0.14	8.62	13.37	13.84	10.10	11.33	9.89	14.76	14.71	14.37	15.20	16.66
Fe_2O_3	12.34±0.06	13.14	13.67	10.47	12.53	13.69	13.44	13.69	14.36	14.27	14.21	13.45
MgO	7.18±0.11	21.10	10.79	7.70	19.04	17.22	16.31	7.99	5.61	5.62	8.49	6.21
CaO	11.37±0.07	7.05	9.49	11.92	7.61	7.67	7.77	9.88	10.12	10.27	9.70	10.22
Na_2O	2.25±0.17	1.41	2.61	2.30	1.74	1.77	1.53	2.58	2.82	3.44	2.34	2.47
K_2O	0.53±0.01	0.31	0.49	0.36	0.13	0.14	0.26	0.35	0.45	0.64	0.26	0.20
TiO_2	2.77±0.01	1.56	2.68	2.24	1.75	2.16	1.83	3.11	3.76	3.72	2.85	2.78
P_2O_5	0.27±0.01	0.17	0.30	0.21	0.18	0.23	0.16	0.35	0.45	0.42	0.30	0.33
MnO	0.17±0.01	0.17	0.18	0.16	0.17	0.17	0.17	0.19	0.21	0.18	0.19	0.19
Sum	100.11±0.41	99.26	100.54	100.43	100.35	100.12	99.41	99.16	99.68	99.47	100.00	99.27
Mg#[c]	56.2	77.9	63.5	61.8	77.0	73.5	72.8	56.2	46.2	46.4	56.8	50.4
H_2O^+	–	0.62	–	–	–	0.77	0.55	0.70	0.75	0.96	1.13	1.43
CO_2	–	0.12	–	–	–	0.23	0.20	0.22	0.44	–	0.37	0.28
Sc	31.8	20.7	26.0	39.3	23.1	22.7	25.8	26.4	29.4	28.9	27.9	26.2
V	286	169	233	283	201	205	205	276	281	291	259	253
Cr	289	1450	402	607	821	582	804	296	103	105	253	222
Co	45.1	96.0	65.9	41.4	80.6	77.4	76.9	54.7	46.7	45.6	59.1	49.6
Ni	115	1073	360	100	925	542	703	184	74	79	226	104
Zn	113	122	119	90	109	122	115	138	122	128	124	142
Rb	9.1	4.9	1.02	5.8	0.81	0.55	4.11	2.1	4.7	–	0.82	0.9
Sr	390	201	392	334	246	308	207	473	508	513	353	386
Ba	135	54	145	90	59	90	57	156	219	209	105	116
Zr	184	101	179	140	108	148	103	218	240	237	187	186
Nb	19.7	7.6	14.92	9.7	7.9	11.9	7.2	17.5	20.1	19.6	13.7	14.1
La	15.5	7.22	13.5	9.23	7.26	10.3	7.1	16.4	19.3	19.7	13.6	12.3
Ce	39.5	18.8	35.6	26.0	19.9	26.5	18.8	42.9	52.1	49.0	34.9	33.5
Nd	24.2	11.8	22.6	17.4	13.4	17.8	12.3	26.9	32.7	30.4	21.8	21.7
Sm	5.93	3.27	6.33	4.97	3.94	4.89	3.73	7.26	8.44	8.70	6.08	6.12
Eu	2.12	1.17	2.12	1.73	1.35	1.86	1.39	2.41	2.87	2.88	2.35	2.17
Tb	0.91	0.59	0.96	0.84	0.60	0.87	0.71	1.08	1.28	1.14	1.10	1.11
Yb	1.96	1.20	2.08	1.87	1.51	1.79	1.73	2.27	2.54	2.65	2.28	2.35
Lu	0.28	0.19	0.29	0.27	0.23	0.24	0.24	0.32	0.37	0.39	0.31	0.33
Hf	4.37	2.4	4.4	3.5	2.7	3.68	2.64	5.2	6.1	5.7	4.6	4.4
Ta	1.13	0.40	0.90	0.59	0.47	0.77	0.51	1.03	1.3	1.3	1.1	0.9
Th	0.95	–	0.6	0.5	0.4	1.0	0.8	1.0	1.4	1.4	0.9	0.8
87/86[d]	0.70347±4	–	–	0.70371	–	0.70382	0.70384	0.70381	0.70379	0.70372	0.70379	0.70380
143/144	0.51301±2	–	–	0.51293	–	0.51292	0.51291	0.51292	0.51295	0.51294	0.51292	0.51293
6/4	18.656	–	–	–	–	–	18.336	–	18.275	18.272	18.245	–
7/4	15.491	–	–	–	–	–	15.479	–	15.476	15.482	15.464	–
8/4	38.198	–	–	–	–	–	38.045	–	37.996	37.993	38.031	–

[a] Samples listed in the order of decreasing age. Major element (wt %) and trace element (V, Ni, Zn, Rb, Sr, Ba, Zr, and Nb) abundances determined by X-ray fluorescence (XRF) method at the University of Massachusetts. H_2O^+ and CO_2 by CHN analyzer (Woods Hole Oceanographic Institute). Abundances of trace elements, Sc, Cr, Co, Rare earth elements, Hf, Ta and Th, determined by neutron activation analyses (NAA) at MIT. Sr, Nd and Pb isotopic ratios determined at MIT. $^{87}Sr/^{86}Sr$ normalized to $^{86}Sr/^{88}Sr=0.1194$ and relative to 0.70800 for E and A standard. $^{143}Nd/^{144}Nd$ normalized to $^{146}Nd/^{144}Nd=0.7219$ and relative to 0.512646 for BCR-1. Pb isotopic ratios normalized relative to $^{206}Pb/^{204}Pb=16.9388$, $^{207}Pb/^{204}Pb=15.4941$, and $^{208}Pb/^{204}Pb=36.7115$, for NBS SRM-981 standard

[b] TH, Tholeiitic picrite and basalt; AB, alkalic basalt, HA, hawaiite; ANK, ankaramite

[c] Mg #: molar MgO/(MgO + FeO) assuming $Fe^{2+}/(Fe^{2+}+Fe^{3+})=0.90$

[d] 87/86: $^{87}Sr/^{86}Sr$; 143/144: $^{143}Nd/^{144}Nd$; 6/4: $^{206}Pb/^{204}Pb$; 7/4: $^{207}Pb/^{204}Pb$; and 8/4: $^{208}Pb/^{204}Pb$

in the Matuyama Reversed-Polarity Chron. The youngest Honomanu lava (HO-12) is normally magnetized, which places it within the Jaramillo Normal-Polarity Subchron, a normal interval within the Matuyama that occurred between 0.91 and 0.98 Ma. The lowermost two Kula lavas in the Honomanu Gulch section (HO-10 and HO-11) are reversely magnetized. Their K-Ar ages are consistent, within analytical uncertainty, with this polarity and place the flows in the latest interval of the Matuyama Reversed-Polarity Chron. The youngest Kula

Honomanu									Kula			Hana
HO-3	HO-4	HO-5	HO-17	HO-16	HO-15	HO-14	HO-13	HO-12	HO-11	HO-10	HO-9	1790
TH	TH	TH	TH	TH	TH	AB	TH	AB	AB	HA	AB	ANK
87	85	83	81	60	57	49	36	32	20	13	6	0
47.70	47.10	47.13	46.41	47.00	46.44	45.98	46.72	46.52	47.20	48.26	45.43	42.62
13.03	13.72	13.85	14.30	13.44	13.33	14.10	15.53	14.09	13.93	15.13	14.69	11.79
13.80	13.49	13.83	13.62	13.30	14.23	13.96	13.76	13.53	14.28	13.14	14.57	14.67
10.44	9.68	9.96	8.52	9.18	9.68	8.21	6.95	8.84	6.11	4.08	6.03	11.72
10.15	10.42	9.93	10.34	10.40	10.26	9.87	10.55	10.18	11.17	8.63	10.30	11.35
2.02	2.45	2.28	2.63	2.42	1.94	2.82	2.53	2.80	2.76	3.86	3.09	2.74
0.30	0.15	0.16	0.26	0.17	0.11	0.43	0.17	0.51	0.57	1.64	1.09	0.82
2.52	2.65	2.63	2.75	2.61	2.69	3.44	2.78	3.04	3.44	4.28	3.80	2.88
0.24	0.26	0.27	0.31	0.26	0.24	0.34	0.29	0.34	0.39	0.79	0.54	0.35
0.19	0.18	0.19	0.20	0.20	0.21	0.20	0.20	0.17	0.20	0.22	0.22	0.22
100.39	100.09	100.18	99.35	98.99	99.13	99.35	99.49	100.02	100.05	100.04	99.75	99.14
62.5	61.2	61.3	57.9	60.3	60.0	56.4	52.7	59.0	48.5	40.6	46.7	63.8
0.59	0.46	0.79	0.48	0.40	0.83	0.60	1.06	0.52	0.25	0.89	0.63	–
0.41	0.40	0.40	0.62	0.26	0.13	0.14	0.16	0.92	0.31	0.32	0.15	–
28.2	30.1	29.8	27.7	29.8	30.4	27.6	29.5	26.4	31.3	20.7	22.9	30.6
262	274	251	235	274	256	278	271	251	311	227	340	339
490	439	428	327	420	563	327	255	295	73	<1	122	606
66.5	58.0	57.5	59.4	57.2	61.9	56.9	54.1	58.1	49.8	40.5	49.7	69.9
360	281	288	214	283	248	226	126	210	82	23	76	265
127	120	117	114	120	121	139	118	116	122	136	127	116
4.39	0.44	0.51	2.6	1.0	0.5	3.0	0.4	5.2	4.8	30.7	20.7	22.7
322	343	324	379	347	326	466	388	486	531	721	746	548
94	92	91	111	100	79	170	110	156	242	539	397	468
158	167	163	179	167	164	207	178	199	235	416	282	170
12.8	14.6	14.5	13.2	14.5	13.4	18.0	13.4	17.1	23.3	50.4	38.2	35.3
10.8	12.5	12.1	12.4	12.3	11.7	15.5	12.6	15.6	19.9	44.0	30.0	22.8
27.7	31.5	31.2	33.2	33.0	31.7	41.7	34.1	41.1	51.5	108	72	53.6
18.5	20.8	20.7	21.9	20.9	20.6	26.0	22.1	24.9	30.2	60.0	40.5	26.8
5.06	5.82	5.49	6.13	5.90	5.87	7.11	6.22	6.82	8.22	13.3	9.12	6.27
1.95	2.02	2.10	2.14	2.12	1.98	2.42	2.20	2.25	2.65	4.17	2.94	2.12
0.90	0.96	0.86	1.07	1.04	0.92	1.10	0.96	0.98	1.07	1.87	1.38	0.97
1.98	2.27	2.15	2.27	2.24	2.13	2.30	2.33	2.05	2.27	3.46	2.37	1.57
0.27	0.31	0.30	0.32	0.32	0.30	0.32	0.36	0.27	0.32	0.48	0.32	0.22
4.1	4.24	4.26	4.4	4.0	4.1	5.0	4.3	4.9	5.6	9.3	6.3	4.1
0.8	1.0	1.0	0.82	0.95	0.88	1.13	0.89	1.00	1.5	3.0	2.44	1.87
0.8	0.9	0.9	0.6	0.6	0.6	0.7	0.5	1.0	1.4	3.2	2.4	1.9
0.70385	0.70384	0.70373	0.70387	0.70385	0.70372	0.70371	0.70365	0.70364	0.70353	0.70337	0.70328	0.70323
0.51295	0.51292	0.51298	0.51293	0.51299	0.51296	0.51297	0.51291	0.51295	0.51301	–	–	0.51305
–	–	–	18.278	–	–	–	–	18.309	18.337			
–	–	–	15.463	–	–	–	–	15.462	15.462			
–	–	–	38.016	–	–	–	–	37.927	37.927			

flow in the gulch (HO-9) is normally magnetized, which indicates that it was probably emplaced during the earliest part of the Brunhes Normal-Polarity Chron, even though its weighted mean K–Ar age is slightly older (0.78 ± 0.01 Ma) than the accepted age of the Brunhes-Matuyama boundary (0.73 Ma).

The K-Ar ages and magnetic polarities show that lavas in the Honomanu Gulch erupted over a period of about 0.37 m.y. Eruptions of the exposed lavas of the Honomanu Basalt began about, or perhaps slightly before, 1.10 Ma and ceased by 0.93 Ma. Eruptions of the Kula Volcanics in the Honomanu Gulch began shortly after 0.93 Ma and continued, with substantial hiatuses, until the beginning of the Brunhes Normal-Polarity Chron at 0.73 Ma. However, Kula volcanism elsewhere on Haleakala continued until about 0.4 Ma (McDougall 1964; Naughton et al. 1980).

Major element composition

The nineteen Honomanu samples range widely in major element composition (e.g., 5.6 to 19.0% MgO, Table 1). They include 3 tholeiitic picrites, 10 tholeiitic basalts, and 6 alkalic basalts (Table 1, Fig. 3), classified according to Macdonald and Katsura (1964). However, as dis-

Table 2. Analytical data for K–Ar age determinations on basalts from Haleakala Volcano, Maui

Sample no.	Material	K_2O (wt %)	Argon			Age (Ma)
			Weight (g)	$^{40}Ar_{rad}$ (10^{-12}mol/g)	$^{40}Ar_{rad}$ (%)	
HO-9	Alkalic basalt	1.101±0.004	10.441	1.016	8.0	0.641±0.042
			10.435	1.416	35.0	0.893±0.026
			9.846	1.228	27.2	0.775±0.024
			9.968	1.185	30.8	0.748±0.023
				Weighted mean=		0.783±0.013
HO-11	Alkalic basalt	0.575±0.003	10.545	0.725	13.4	0.876±0.053
			10.239	0.924	8.6	1.117±0.061
			3.126	0.378	5.6	0.457±0.127
				Weighted mean=		0.93 ±0.33
HO-12	Alkalic basalt	0.497±0.002	11.151	0.669	13.5	0.936±0.066
			10.053	0.711	20.1	0.994±0.060
				Weighted mean=		0.968±0.044
HO-21	Tholeiitic basalt	0.355±0.005	10.823	0.952	5.8	1.860±0.150
			10.319	0.482	6.4	0.943±0.095
			9.874	0.570	7.7	1.116±0.084
			10.187	0.504	7.2	0.986±0.082
				Weighted mean=		1.104±0.047

Note: Ages calculated using 1976 IUGS constants (Steiger and Jäger 1977): $L_\beta = 4.962 \times 10^{-10}yr^{-1}$, $L_\varepsilon = 0.581 \times 10^{-10}yr^{-1}$, $^{40}K/K_{total} = 1.167 \times 10^{-4}$ mol/mol. Errors are estimates of analytical precision at the 68% confidence level. Weighted means and errors are calculated following Taylor (1982) except for HO-11 where the error is the calculated standard deviation (not weighted) of the three measurements. K_2O values are the means of four independent analyses

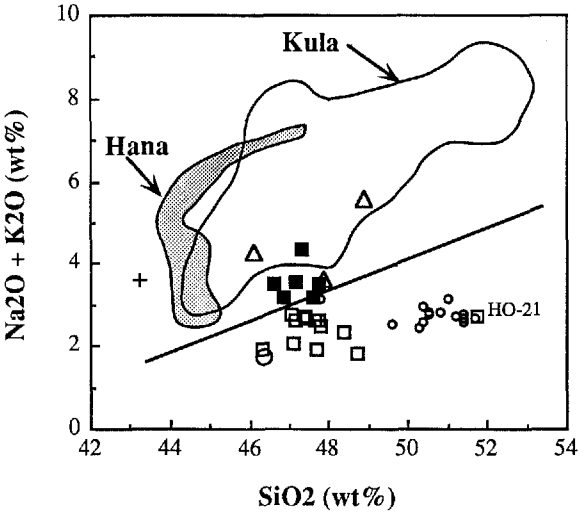

Fig. 3. Variation of Na_2O+K_2O with SiO_2 in Haleakala lavas. *Open square*, tholeiite from the Honomanu Basalt; *filled square*: alkalic basalt from the Honomanu Basalt; *open triangle*, alkalic basalt and hawaiite from the Kula Volcanics; *cross*: ankaramite from the Hana Volcanics; *open circles*: dredge samples from east rift zone of Haleakala (*large symbol* for sample in Table 1; *smaller symbols* are for the dredge glasses reported by Moore et al. 1990). In order to make the alkali-SiO_2 data in Table 1 consistent with the tholeiite-alkalic basalt boundary line (the *solid straight line*) proposed by Macdonald and Katsura (1964), Fe_2O_3 was converted to FeO and oxides were normalized to 100%. In this and subsequent figures (except Fig. 11) the fields for Kula and Hana lavas from the Nahiku drill cores are shown (data from Chen and Frey 1985; Chen et al. 1990). The oldest Kula sample from the Honomanu Gulch (HO-11) has a lower total alkali content than the Kula samples from drill cores. The 1790 Hana lava flow has a lower SiO_2 content than the Hana samples from drill cores

cussed later the K_2O contents in some samples were decreased by up to ~0.2% during post-magmatic alteration; therefore, compositional changes caused by alteration slightly increased the tholeiitic character of these samples. Nevertheless, the most important observations are the continuous transition between tholeiitic and alkalic lavas in an alkali versus SiO_2 diagram (Fig. 3), and the intercalation of tholeiitic and alkalic basalt flows in the Honomanu Basalt (Fig. 2).

Among Honomanu tholeiitic and alkali lavas there is overlap in MgO, Al_2O_3, Fe_2O_3 and CaO abundances (Fig. 4a–d), and in CaO/MgO, Al_2O_3/CaO and K_2O/P_2O_5 ratios (Fig. 5a–c). However, relative to the tholeiitic lavas, the alkalic lavas have higher abundances of alkali metals, TiO_2 and P_2O_5 (Fig. 4e–h). At similar MgO contents, subaerial Honomanu lavas (except sample HO-21) have lower SiO_2 and CaO contents, but higher Al_2O_3 and Fe_2O_3 contents than those reported for submarine glasses from the east rift of Haleakala (Haleakala Ridge, Moore et al. 1990) (Fig. 4a–d). Sample HO-21 (7.7% MgO), which is from the lower section of the subaerial part of the Honomanu Basalt (Fig. 2), has a major element composition similar to some of the Haleakala submarine glasses (Figs. 3 and 4). The dredge sample (KK83-0725), also from the east rift zone of Haleakala, has significantly lower bulk rock SiO_2, Al_2O_3, CaO, Na_2O, and TiO_2 contents, but higher MgO content than the submarine glasses (Figs. 3 and 4). Compared to the Honomanu samples, the dredge sample has higher MgO, lower Al_2O_3, CaO and TiO_2 contents, but similar SiO_2, Fe_2O_3, Na_2O, K_2O and P_2O_5 contents (Fig. 4a–h).

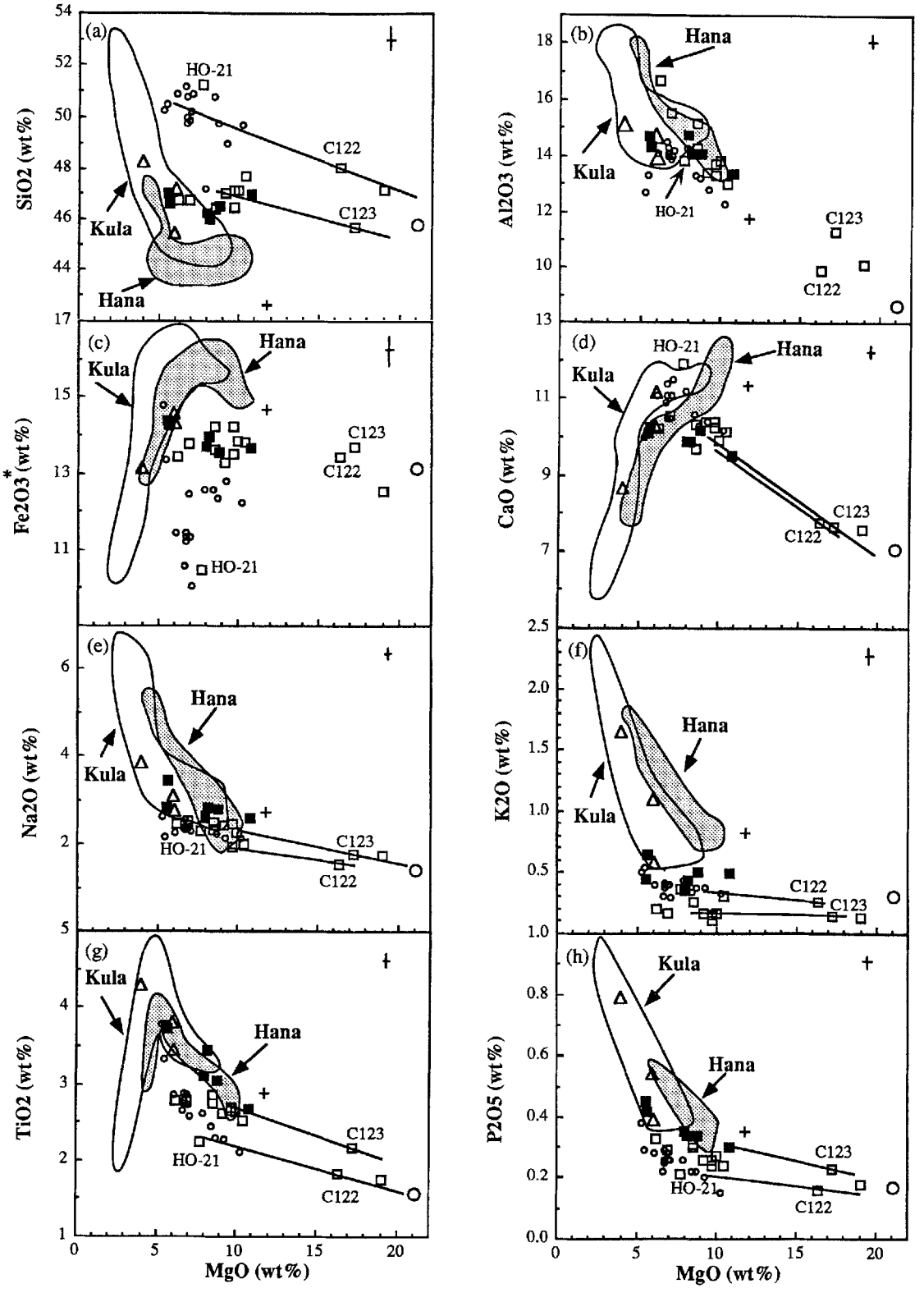

Fig. 4a–h. Variations of major oxides: **a** SiO_2, **b** Al_2O_3, **c** Fe_2O_3* (total iron as Fe_2O_3), **d** CaO, **e** Na_2O, **f** K_2O, **g** TiO_2 and **h** P_2O_5 with MgO of Haleakala samples. *Symbols* as in Fig. 3. Olivine (Fo_{82}, the olivine phenocryst composition in C122) control lines are shown for two assumed parental melts, C122 and C123. Cross on the *upper right corner* of the diagrams represents $\pm 2\,\sigma$ analytical uncertainty for the whole-rock samples

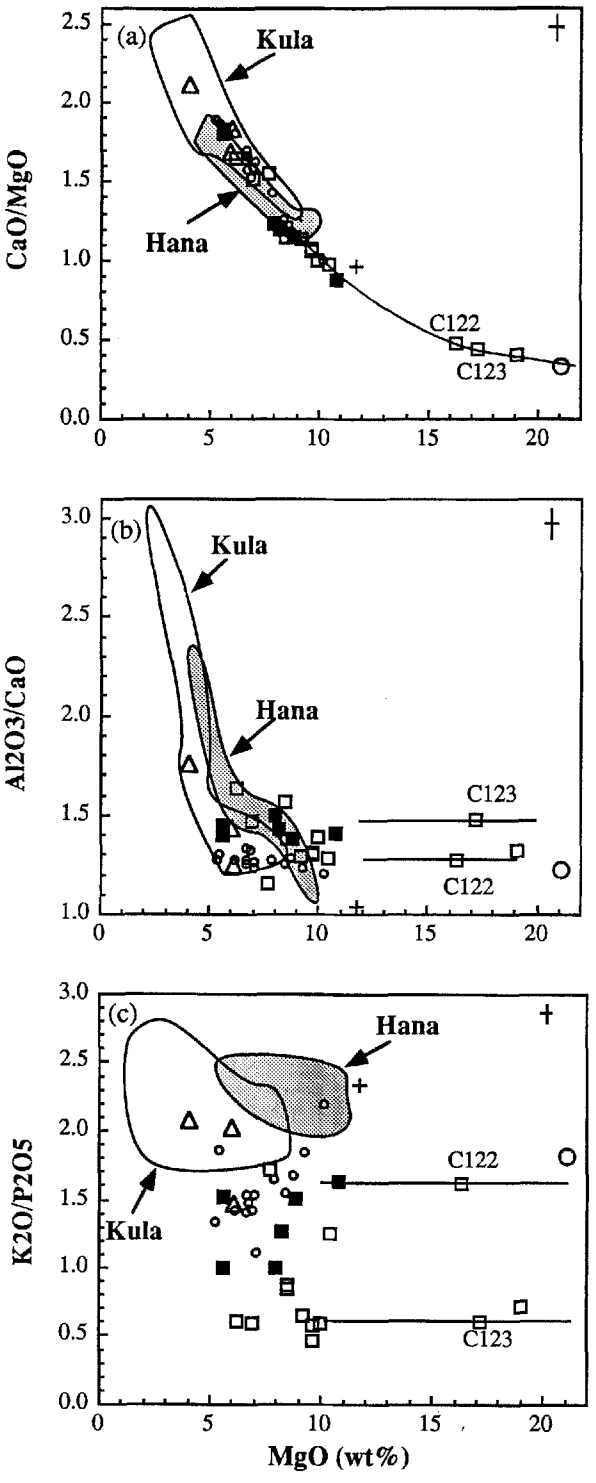

Fig. 5a–c. Variations of **a** CaO/MgO, **b** Al_2O_3/CaO and **c** K_2O/P_2O_5 as a function of MgO content in Haleakala samples. *Symbols* as in Fig. 3. *Cross* on the upper right corner of the diagrams represents $\pm 2\sigma$ analytical uncertainty

Most of the Honomanu samples have K_2O/P_2O_5 ratio less than 1.3 and this contrasts with K_2O/P_2O_5 ratios greater than 1.3 in all but one submarine glasses from Haleakala (Fig. 5c) (Moore et al. 1990) and recent subaerial basalts from Kilauea and Mauna Loa (Wright 1971). As previously concluded for subaerial lavas from Kohala (Feigenson et al. 1983) and Mauna Kea (Frey et al. 1990), we infer that the low K_2O/P_2O_5 ratio in most Honomanu lavas reflects the effects of post-magmatic subaerial alteration.

Major element compositions of the three Kula samples from the Honomanu Gulch (Table 1) are within the ranges reported for Kula samples from drill cores (Fig. 4; Chen et al. 1990), except for the lower total alkali content in the oldest Kula sample, HO-11 (Fig. 3). The youngest Hana sample (sample 1790, Table 1) has a higher MgO content, but lower SiO_2 and Al_2O_3 contents than those reported for Hana samples from drill cores (Figs. 3 and 4; Chen et al. 1990).

Transition metals (Sc, V, Cr, Cr, Ni, and Zn)

Abundances of Cr, Co and Ni are highly variable in Honomanu lavas, and their abundances correlate positively with MgO content (Fig. 6c–d). In contrast, abundances of Sc, V and Zn are less variable, with Sc and V contents varying inversely with MgO content (Fig. 6a–b). In these MgO variation plots there are no obvious differences between alkali and tholeiitic Honomanu lavas. The dredge sample (KK83-0725) has lower Sc, and V contents, but higher Cr, Co, and Ni contents than the Honomanu samples (Table 1, Fig. 6a–d). In Sc, V, Co and Ni versus MgO plots, the three Kula samples plot within the fields reported for the drill core Kula samples (Fig. 6a–d). However, the Hana sample (1790) contains higher Co and Ni contents than the drill core Hana samples (Fig. 6c–d), which is consistent with its high MgO content.

Incompatible trace elements (P, Rb, Sr, Ba, Zr, Hf, Nb, and REE)

Abundances of incompatible elements in Honomanu lavas vary by factors of 3.8 (Ba), 2.8 (P_2O_5, Nb, La, and Ce), 2.7 (Nd), 2.5 (Sr), 2.3 (Zr, Hf, and Sm), and 2.1 (Eu) with the lowest abundances in a tholeiitic picrite (C122), and the highest abundances in the most evolved alkalic basalts (HO-19 and C124) (Table 1, Fig. 7). Although some tholeiitic basalts have lower MgO contents than some alkalic basalts, all of the tholeiitic lavas have lower abundances of the incompatible elements, Sr, Ba, Nb, La, Ce, Nd, and Sm, than the alkalic lavas (Table 1, Fig. 7). The dredged picrite (KK83-0725) and C122 have similar abundances of highly incompatible elements, but the dredged sample has lower abundances of intermediate to heavy REE (Sm through Lu; Table 1).

The abundances of heavy REE (Yb and Lu) vary by a factor of 1.7 in Honomanu lavas (Table 1). If only the mafic samples (MgO $\geq$ 7%) are considered, the abundances of light REE (e.g., La) and heavy REE (e.g., Yb) vary by factors of 2.2 and 1.5, respectively (Table 1). However, after correction for olivine fractionation, La abundances in the fractionation-corrected mafic lavas vary by a factor of 1.7, whereas Yb abundances vary by only a factor of 1.1.

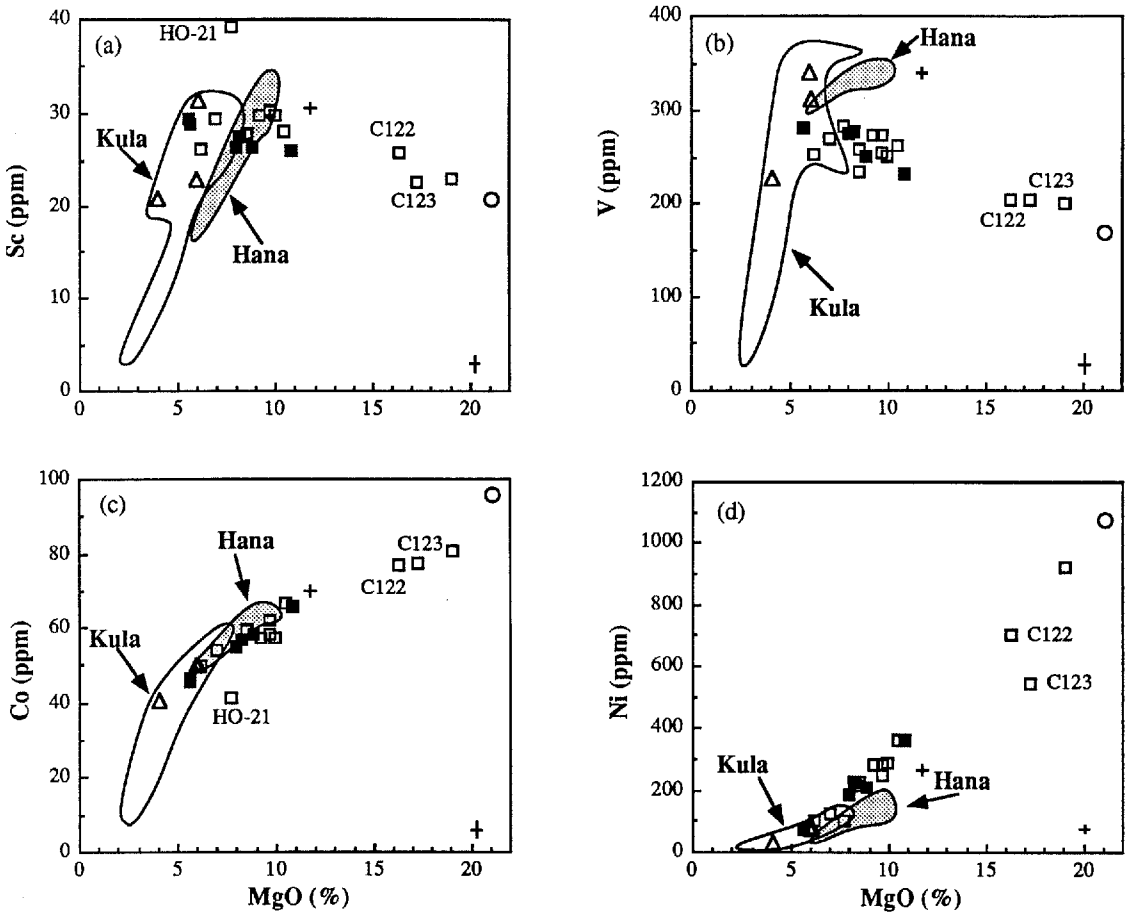

Fig. 6a–d. Variations of transition metals **a** Sc, **b** V, **c** Co, and **d** Ni as a function of MgO content in Haleakala samples. Symbols as in Fig. 3. *Cross* on the lower right corner of the diagrams represents $\pm 2\,\sigma$ analytical uncertainty

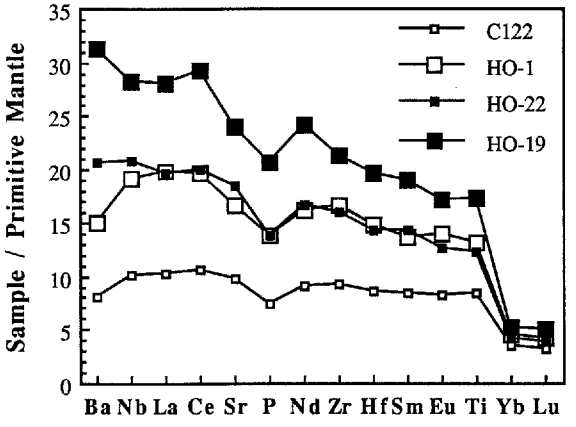

Fig. 7. Primitive mantle normalized trace element distributions (Sun and McDonough 1989) of tholeiitic and alkalic lavas of the Honomanu Basalt. *Open symbols*: range for tholeiitic lavas (lower and upper limits defined by samples C122 and HO-1, respectively); *filled symbols*: range for Honomanu alkalic lavas (lower and upper limits defined by samples HO-22 and HO-19, respectively). All Honomanu alkalic lavas have higher incompatible element abundances than the tholeiitic lavas

All Honomanu lavas have LREE-enriched chondrite-normalized or primitive-mantle-normalized patterns (Fig. 7). Abundance ratios of LREE elements (e.g., La/Ce, La/Nd) are very similar for Honomanu tholeiitic and alkalic lavas. For example, $(La/Ce)_N$ (N in the subscript indicates chondrite normalized) ranges from 0.92 to 1.02 for the tholeiites, and 0.96 to 1.03 for the alkalic basalts. However, the alkalic basalts have higher LREE/intermediate REE (e.g., La/Eu) and LREE/HREE ratios (e.g., La/Yb) than the tholeiites (Figs. 8 and 9). For example, $(La/Eu)_N$ and $(La/Yb)_N$, range from 1.25 to 1.52 and 2.94 to 4.28, respectively, in the tholeiitic lavas, and from 1.57 to 1.69 and 4.83 to 5.46, respectively, in the alkalic lavas.

Sr, Nd and Pb isotopic ratios

The $^{87}Sr/^{86}Sr$ ratios of Honomanu lavas (17 samples, this paper; 2 samples from West and Leeman 1987) range from 0.70364 to 0.70387 and are significantly higher than the $^{87}Sr/^{86}Sr$ ratios in Kula and Hana lavas (Fig. 10a). The $^{143}Nd/^{144}Nd$ ratios of Honomanu lavas (17 samples) range from 0.51291 to 0.51299 and are lower than $^{143}Nd/^{144}Nd$ ratios in younger Kula and Hana lavas (Fig. 10a). The range of $^{87}Sr/^{86}Sr$ in Hono-

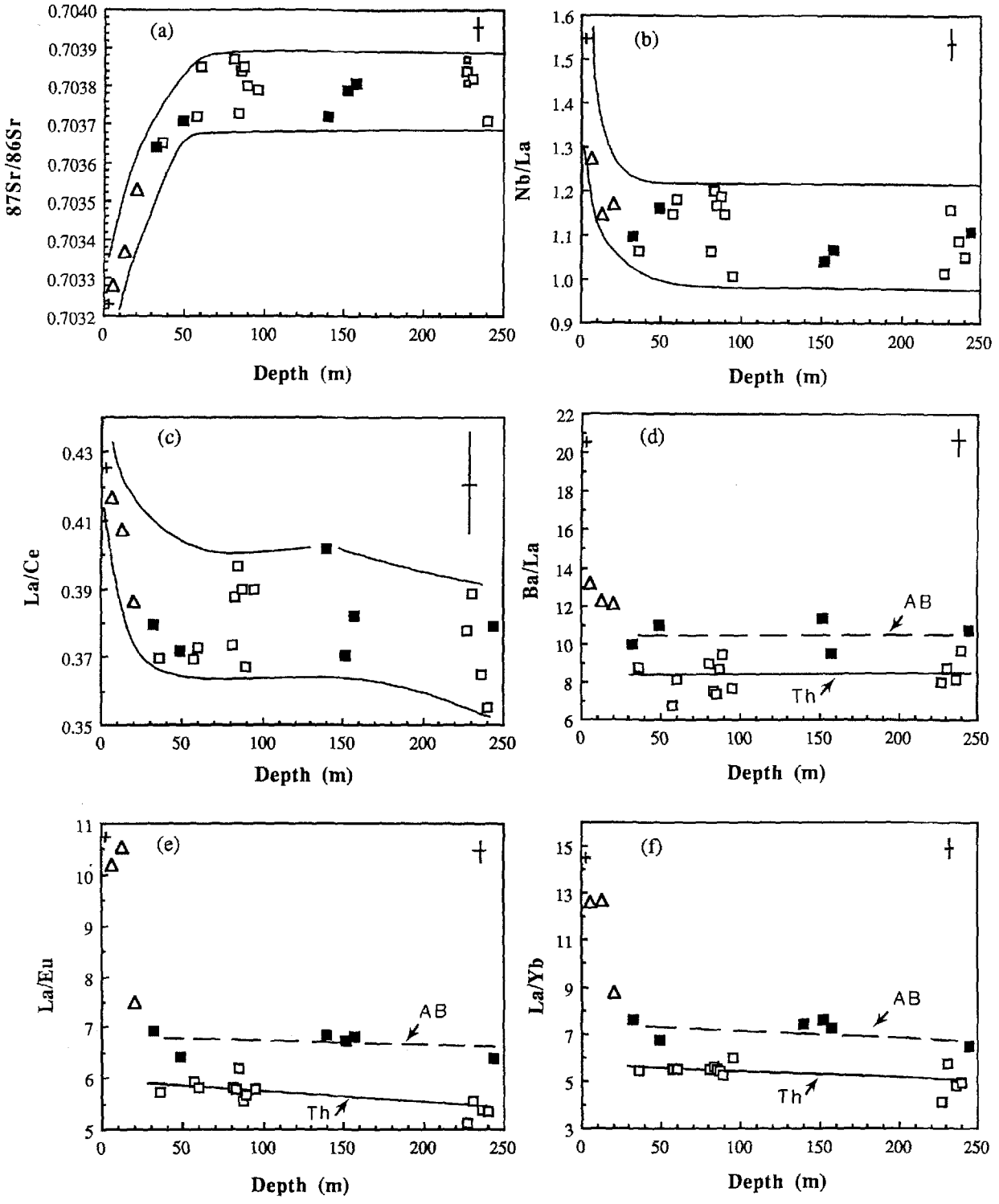

Fig. 8a–f. Variations of **a** $^{87}Sr/^{86}Sr$, the two *small squares* above and below a large *open square* represent duplicate analyses of sample C122, **b** Nb/La, **c** La/Ce, **d** Ba/La, **e** La/Eu, and **f** La/Yb, as a function of stratigraphic depth. *Symbols* as in Fig. 3. The tholeiitic lavas of the Honomanu Basalt have the same ranges of $^{87}Sr/^{86}Sr$, Nb/La, and La/Ce ratios as the Honomanu alkalic lavas. However, all the Honomanu alkalic lavas have higher Ba/La, La/Eu, and La/Yb than the tholeiitic lavas (variation trends for tholeiitic and alkalic samples are shown as *solid line* and *dashed line*, respectively). *Cross* on the upper right corner of the diagrams represents $\pm 2\sigma$ analytical uncertainty

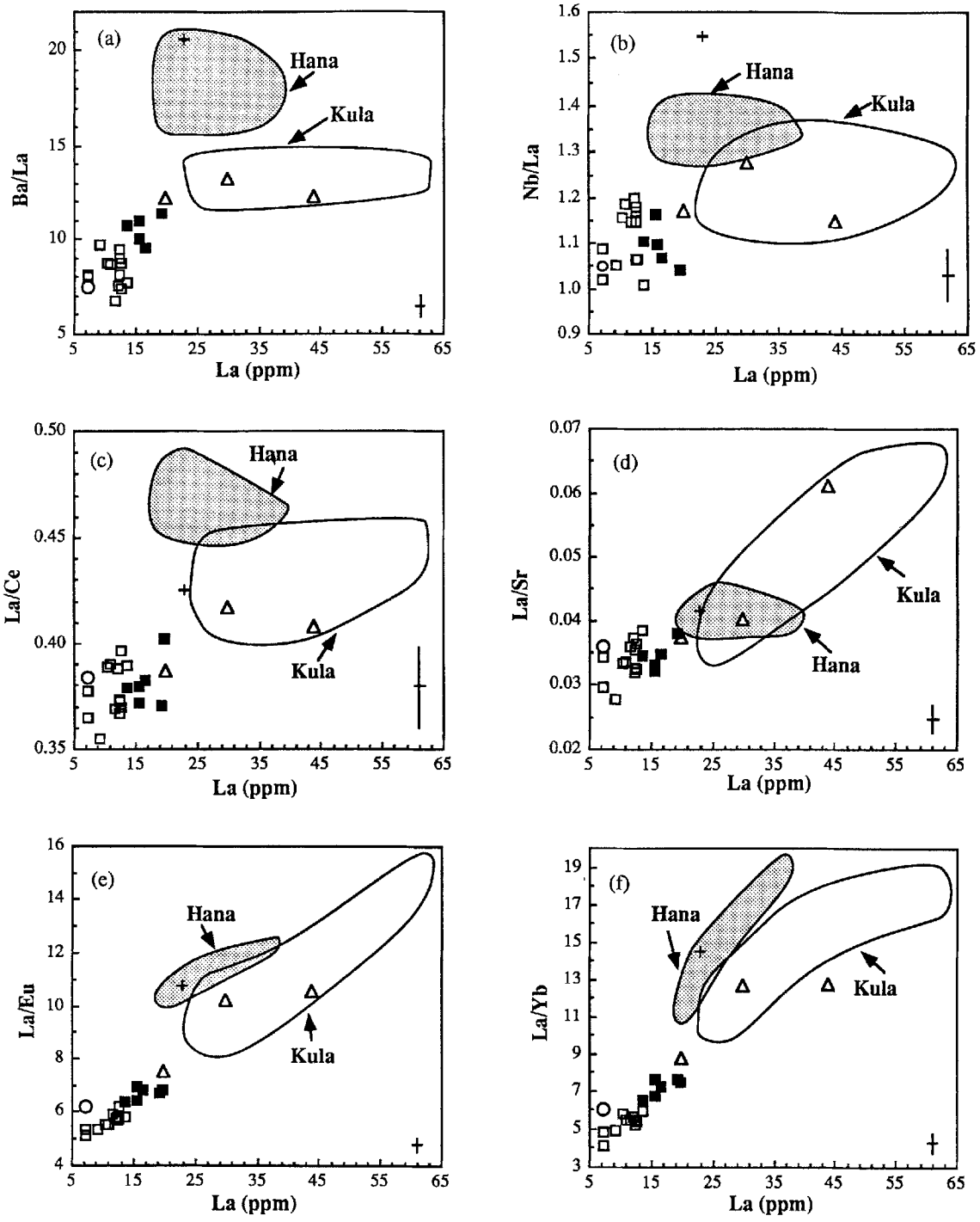

Fig. 9a–f. Variations of **a** Ba/La, **b** Nb/La, **c** La/Ce, **d** La/Sr, **e** La/Eu, and **f** La/Yb ratios with La abundances in the Haleakala lavas. *Symbols* as in Fig. 3. *Cross* on the lower right corner of the diagrams represents $\pm 2\,\sigma$ analytical uncertainty

manu lavas is about three times $\pm 2\,\sigma$ analytical errors (Fig. 10a). The range of $^{143}Nd/^{144}Nd$ ratios in Honomanu lavas are slightly larger than the $\pm 2\,\sigma$ analytical error (95% confidence level), but is within the $\pm 3\,\sigma$ analytical error (99.7% confidence level).

A significant new result is that the uppermost Honomau lavas, tholeiitic lava HO-13 and alkalic lava HO-12 (Fig. 2), have $^{87}Sr/^{86}Sr$ ratios (0.70365 and 0.70364, respectively) lower than stratigraphically lower Honomanu lavas (0.70372 to 0.70387, Fig. 10a). In addition, the oldest dated Kula lava, HO-11 (0.93 ± 0.04 Ma), has an $^{87}Sr/^{86}Sr$ ratio of 0.70353 which is higher than the range, 0.70308 to 0.70347, for 38 previously analyzed Kula lavas (Fig. 10a; Chen and Frey 1985; West and Leeman 1987; Chen et al. 1990). Therefore, the youngest Honomanu and oldest Kula lavas define a gradual temporal decline in $^{87}Sr/^{86}Sr$. Additional support for this temporal variation is the range of Sr isotope ratios, 0.70345 to 0.70355 in 5 lavas from the Kumuiliahi Formation (West and Leeman 1987). This sequence of lavas

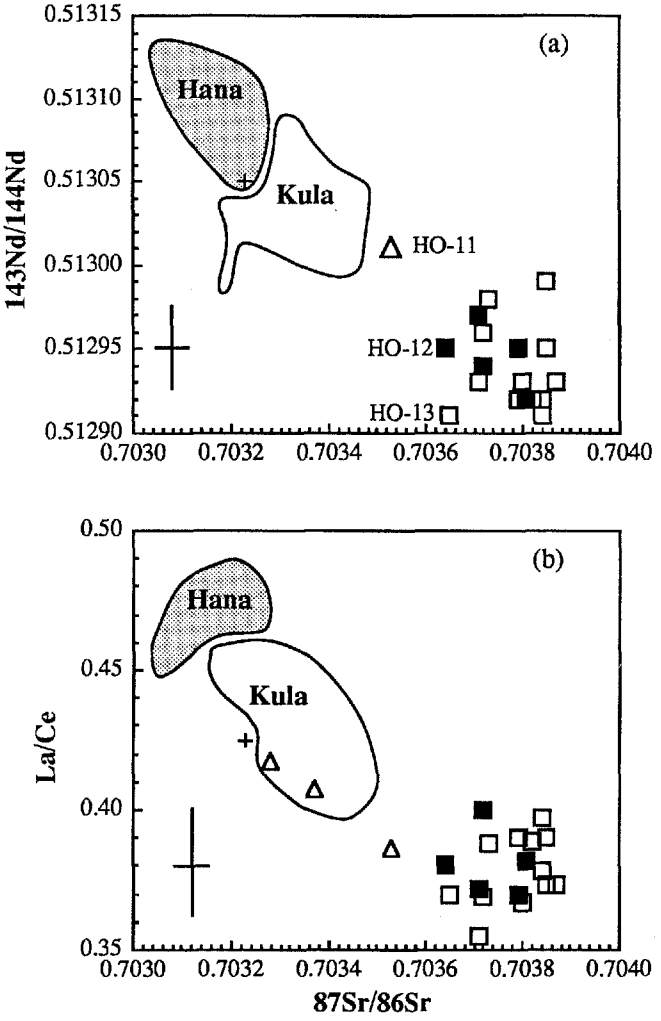

Fig. 10a, b. Correlation of **a** $^{143}Nd/^{144}Nd$ and **b** La/Ce ratios with $^{87}Sr/^{86}Sr$ ratios in the Haleakala lavas. *Symbols* as in Fig. 3. The *cross* in the lower left corner represents $\pm 2\,\sigma$ analytical uncertainty

is exposed only in Haleakala crater and overlaps in K–Ar ages (0.70 to 0.91 Ma, McDougall 1964; Naughton et al. 1980) and $^{87}Sr/^{86}Sr$ with the lower lavas of the Kula Volcanics (Fig. 10).

Although all Hana lavas have relatively low $^{87}Sr/^{86}Sr$ (0.70306 to 0.70329 for 10 lavas; Chen and Frey 1985; West and Leeman 1987; Chen et al. 1990), there is no systematic change in the $^{87}Sr/^{86}Sr$ of Hana lavas with stratigraphic position. This result is corroborated by the relatively high $^{87}Sr/^{86}Sr$ ratio, 0.70323, in the youngest (~1790 AD) Hana lava (Table 1, Fig. 10a).

The $^{206}Pb/^{204}Pb$, $^{207}Pb/^{204}Pb$ and $^{208}Pb/^{204}Pb$ ratios of the Honomanu lavas (6 samples, this study; 2 samples from West and Leeman 1987) range from 18.245 to 18.336, 15.461 to 15.482 and 37.919 to 38.045, respectively (Fig. 11a–b). The range of $^{206}Pb/^{204}Pb$ ratios in the Honomanu lavas (~2.5 times $\pm 2\,\sigma$) is larger than the 95% confidence level of analytical error ($\pm 2\,\sigma$). However, the ranges of $^{207}Pb/^{204}Pb$ and $^{208}Pb/^{204}Pb$ ratios in the Honomanu lavas are within the ± 2 sigma analytical errors (Fig. 11a–b). In contrast, the Kula lavas (5 samples, Tables 1 and 3; 17 samples, West and Leeman 1987) define larger ranges in Pb isotopes (Fig. 11a–b). As a result, Honomanu, Kula, and Hana lavas define overlapping fields in Pb–Pb plots, and there are no long-term, systematic temporal trends in Pb isotopic ratios. However, because of their higher $^{87}Sr/^{86}Sr$ ratios, Honomanu lavas define a field which does not overlap with the Kula and Hana fields in $^{87}Sr/^{86}Sr$ versus $^{206}Pb/^{204}Pb$ and $^{87}Sr/^{86}Sr$ versus $^{208}Pb/^{204}Pb$ plots (Figs. 11c–d). This offset of older tholeiitic and alkalic lavas to higher $^{87}Sr/^{86}Sr$ at a given $^{206}Pb/^{204}Pb$ is characteristic of mature Hawaiian volcanoes that have erupted relatively young postshield and/or posterosional lavas (Chen 1987; West et al. 1987). The temporal trend of $^{87}Sr/^{86}Sr - ^{206}Pb/^{204}Pb - ^{208}Pb/^{204}Pb$ at individual Hawaiian volcanoes has been interpreted as a result of mixing between enriched component(s) and a depleted MORB-related component (Chen 1987; West et al. 1987).

Discussion

Compositional effects of crystal segregation and accumulation

The two Honomanu tholeiites with ~16 to 17% MgO have been proposed as possible primary melts (C122, Chen 1990; and C123, Maaloe and Hansen 1982). These two samples have very different compositions (Table 1). Sample C123 has lower abundances of SiO_2 (Fig. 4a) and compatible trace elements, Sc, Cr, and Ni (Fig. 6a and d), but higher abundances of TiO_2, P_2O_5 and incompatible trace elements, and a higher Al_2O_3/CaO ratio (1.27 for C122, 1.48 for C123) (Fig. 5b). These compositional differences are consistent with derivation of sample C123 by a smaller degree of melting. Olivine fractionation from a parental magma composition like sample C123 could explain most of the major element abundance variations (samples HO-18 and HO-21 are exceptions) in the Honomanu tholeiites (Figs. 4 and 5). However, sample HO-18, the tholeiite with the lowest MgO content (6.2%) has a high Al_2O_3/CaO (1.63, Fig. 5b) and a relatively low Sc content (Fig. 6a). These compositional features probably reflect the onset of clinopyroxene fractionation. Sample HO-21 (7.7% MgO), which has the highest SiO_2 content among the Honomanu samples, is similar to the submarine glasses in major element composition (Figs. 3–5). Based on major element trends, C122 is a likely parental melt for sample HO-21 and the submarine glasses (Figs. 4 and 5).

Among the six Honomanu alkalic basalt samples studied, four have MgO contents ranging from ~8 to 10.8%. Although at a given MgO content these alkalic lavas have higher contents of Na_2O, K_2O, TiO_2 and P_2O_5 than the tholeiitic basalts (Fig. 4e–h), the trends for other major elements and compatible trace elements are similar for the alkalic and tholeiitic basalts (Figs. 4–6). Compared to the most evolved tholeiitic lavas (e.g., HO-18), the most evolved alkalic lavas, HO-19 and C-124 (5.6% MgO) have lower Al_2O_3 abundances, and lower Al_2O_3/CaO ratios, but higher Sc contents (Figs. 5

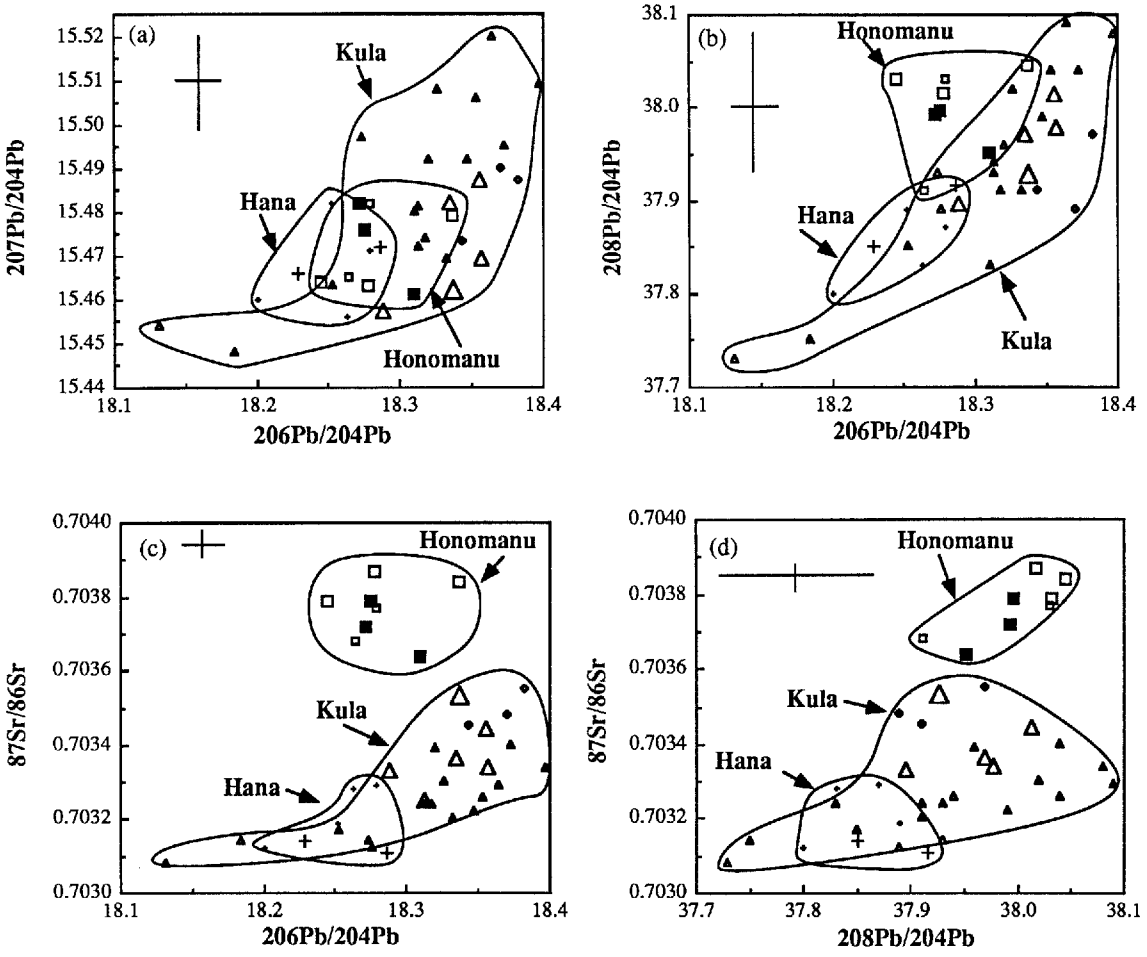

Fig. 11a–d. Variations of Pb isotopic ratios in the Haleakala lavas. **a** Correlation of $^{207}Pb/^{204}Pb$ with $^{206}Pb/^{204}Pb$, **b** correlation of $^{208}Pb/^{204}Pb$ with $^{206}Pb/^{204}Pb$, **c** correlation of $^{87}Sr/^{86}Sr$ with $^{206}Pb/^{204}Pb$, and **d** correlation of $^{87}Sr/^{86}Sr$ with $^{208}Pb/^{204}Pb$. The *crosses* represent ± 2 sigma analytical uncertainty. *Symbols* as in Fig. 3. Pb isotopic data for six Honomanu samples and one Kula sample are in Table 1 (*large symbols*). Additional new data for four Kula and two Hana samples (also shown as *large symbols*) are in Table 3. *Smaller symbols* are for samples reported in West and Leeman (1987). The *diamonds* are for samples from Kumuiliahi Formation (West and Leeman 1987). Kumuiliahi basalt flows have K–Ar ages similar to the lower and middle parts of the Kula Volcanics (Table 2; McDougall 1964; Naughton et al. 1980); therefore they are included in the Kula Volcanics. *Cross* in the *upper left corner* of the diagrams represents $\pm 2\,\sigma$ analytical uncertainty

Table 3. Pb isotopic ratios of lavas from Kula and Hana Volcanics, Haleakala[a]

	Kula Volcanics				Hana Volcanics	
Sample	H85-1	H85-10	H65-4	H85-22	H65-11	H65-13
Rock type	AB	AB	AB	AB	ANK	ANK
$^{206}Pb/^{204}Pb$	18.356	18.335	18.357	18.288	18.229	18.286
$^{207}Pb/^{204}Pb$	15.487	15.482	15.469	15.457	15.466	15.472
$^{208}Pb/^{204}Pb$	38.014	37.970	37.987	37.896	37.851	37.916

[a] Normalization values for Pb isotopes are the same as those listed in the footnote of Table 1. Sr isotopic ratios of these samples can be found in Chen and Frey (1985)

and 6). If the primary magmas for tholeiitic and alkalic Hawaiian basalts have a similar major element composition (Feigenson et al. 1983), the plagioclase/clinopyroxene ratios were higher in the fractionating assemblage that led to the evolved alkalic lavas.

A compositionally homogeneous source for Honomanu tholeiitic and alkalic lavas?

Sr isotope ratios in the lavas from the lower 200 meters of the Honomanu section are quite constant (0.70387 to 0.70371), with no temporal trend or systematic differences between tholeiitic and alkalic lavas (Fig. 8a). Only the uppermost Honomanu lavas, HO-12 and HO-13 are distinct in $^{87}Sr/^{86}Sr$ (Fig. 8a). This temporal decrease in $^{87}Sr/^{86}Sr$ continues into the overlying Kula lavas (Fig. 8a) and provides evidence for a significant change in source composition, perhaps a change in mixing proportions of different source components, that coincides with the transition from Honomanu Basalt to Kula Volcanics (Chen and Frey 1983, 1985). Because of the small range in Nd and Pb isotopic ratios in the Honomanu Basalt (Figs. 10a and 11), no temporal trend is discernible. Consequently, Sr, Nd and Pb isotopic data for Honomanu lavas from the depth region of 250 to 50 meters show that the sources of the intercalated tholeiitic and

alkalic lavas were similar with very little isotopic heterogeneity.

In basaltic lavas abundance ratios involving elements of similar incompatibility, e.g., Nb/La, La/Ce, P/Nd, Hf/Sm and Zr/Hf, are not significantly affected by fractional crystallization; therefore these ratios may reflect the source composition. Specifically, the good correlation of La/Ce ratio with $^{87}Sr/^{86}Sr$ in Haleakala lavas (Fig. 10b) shows that this ratio reflects mantle source components. Moreover, several of these ratios are quite constant throughout the stratigraphic section of Honomanu lavas (e.g., Fig. 8b–c). For example, Nb/La, La/Ce, La/Sr, Hf/Sm, Zr/Hf, and Ti/Eu ratios in the intercalated Honomanu tholeiitic and alkalic lavas are 1.1 ± 0.1 ($\pm 2\sigma$), 0.38 ± 0.02, 0.034 ± 0.005, 0.72 ± 0.08, 40 ± 2, and 7700 ± 600, respectively. Apparently, the mantle source(s) for Honomanu tholeiitic and alkalic lavas had relative abundances of highly incompatible non-volatile elements (e.g., Nb, La, Ce, Sr, Zr, Hf, Sm, Eu, Ti) very similar to estimates of primitive mantle composition (e.g., $(Nb/La)_N = 1.1$, $(La/Ce)_N = 1.03$, $(La/Sr)_N = 1.03$, $(Hf/Sm)_N = 1.03$, $(Zr/Hf)_N = 1.1$ and $(Eu/Ti)_N = 1.0$) (Fig. 7). However, the overlying younger Kula and Hana lavas are significantly enriched in the most incompatible elements; e.g., they have relatively high Nb/La, La/Ce, and La/Sr (Figs. 8 and 9). P/Nd ratios in the tholeiites and alkalic basalts are also quite constant thoughout the Honomanu Basalt and average to 58 ± 7 ($\pm 2\sigma$). This P/Nd ratio is lower than that estimated for the primitive mantle (70, Sun and McDonough 1989), but is similar to that in lavas from other Hawaiian volcanoes (Frey et al. 1990). In contrast, abundances ratios involving alkali elements vary widely in the Honomanu Basalt. For example, Rb/Ba varies from 0.006 to 0.07, K/La varies from 78 to 324, and Rb/Sr varies from 0.001 to 0.02 for Honomanu tholeiitic and alkalic lavas. These wide ranges reflect loss of alkalis during late stage alteration (Feigenson et al. 1983; Chen and Frey 1985; Frey et al. 1990).

Constraints on the partial melting process which generated the Honomanu tholeiitic and alkalic lavas

Because isotopic ratios and highly incompatible element abundance ratios indicate that the intercalated Honomanu tholeiitic and alkalic lavas were derived from compositionally similar sources, the compositional differences between the tholeiitic and alkalic lavas (Figs. 4–9) must have resulted from differences in partial melting and/or post-melting crystal fractionation processes. The specific compositional differences that must be explained are: (a) at similar MgO contents, the alkalic basalts have higher K_2O, TiO_2 and P_2O_5 contents than the tholeiitic basalts (Fig. 4); (b) regardless of their MgO content, all alkalic Honomanu lavas have higher Sr, Ba, Zr, Nb, Hf, and LREE abundances than the tholeiites (Fig. 7); and (c) Nb/Zr, La/Sm, La/Eu and La/Yb ratios to not correlate with MgO contents, but they correlate with abundances of highly incompatible elements, such as La (e.g., Fig. 9e–f). Crystal fractionation alone could not have created these differences between the tholeiitic and alkalic Honomanu lavas. However, these trends of incompatible element abundances could be explained by lower degrees of partial melting for alkalic lavas.

Incompatible element abundances in parental melts can provide constraints regarding the range in degree of partial melting which generated the Honomanu lavas. As discussed earlier, much of the major element variation in mafic Honomanu lavas ($MgO \geq 7\%$) may be explained by olivine fractionation. Parental magma compositions were calculated by addition or subtraction of olivine to form parental magmas with 17.2% MgO; i.e. comparable to the high MgO lava, C123. The abundances of incompatible elements (Ba, Nb, La, Ce, Sr, P, Nd, Zr, Hf, Sm, Eu, Ti, Yb, and Lu) in these calculated parental melts of the mafic Honomanu tholeiitic lavas are between those of C122 ($La/Yb = 4.1$) and C123 ($La/Yb = 5.8$) (Fig. 12a–b). Therefore, the range of partial melting in tholeiitic Honomanu lavas can be defined by these two picrites (C122 and C123). Abundances of highly incompatible elements in C123 are about 1.5 times those in 122 (1.6 for Ba and Nb, 1.5 for La and Sr, and 1.4 for Ce, P, Nd, Zr and Hf; Fig. 12b). Therefore,

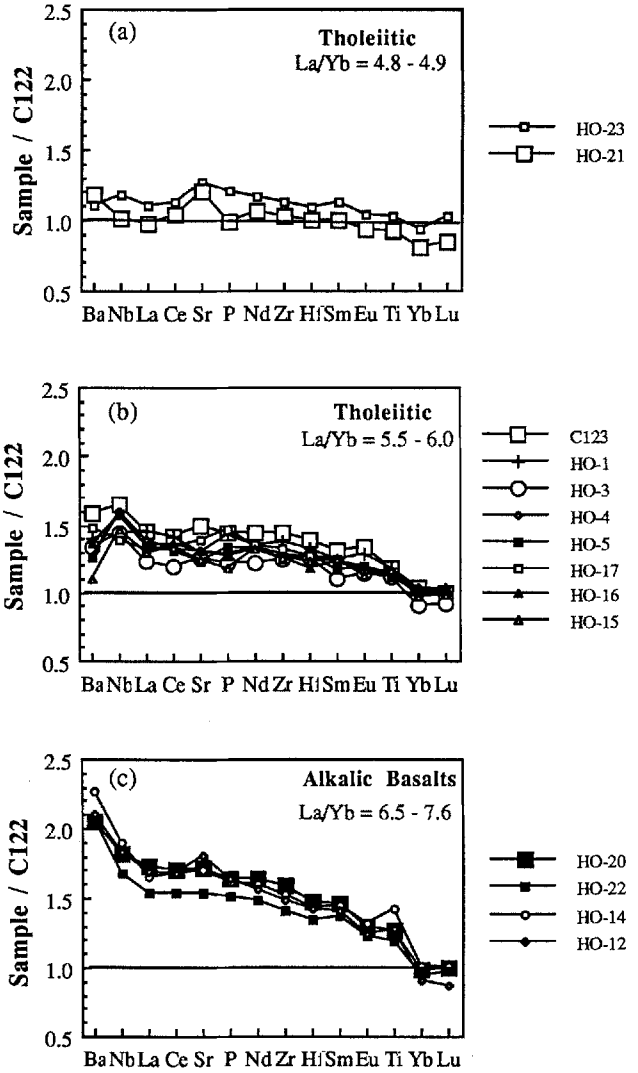

Fig. 12. Olivine fractionation-corrected (corrected to 17.2% MgO by addition or subtraction of equilibrium olivine) trace element abundances in mafic Honomanu lavas ($MgO > 7\%$) relative to sample C122

the range of tholeiitic compositions formed from variable degrees (~a factor of 1.5) of melting.

The best samples for inferring the difference in the degrees of partial melting which generated tholeiitic and alkalib basalts are those that were derived from the same mantle source (e.g., same isotopic ratios) and have undergone similar degree of fractionation (i.e., similar MgO contents, and plot on the same major element variation trends). Sample HO-1 (a tholeiite with Mg # = 56.8) and sample HO-20 (alkalic basalt with Mg # = 56.2) may serve this purpose. Abundances of highly incompatible elements in HO-20 are about 20% (Nb, La, Ce, and Nd) to ~50% (Ba) higher than in HO-1. Therefore, the degree of partial melting which generated the Honomanu alkali basalts may have been about a factor of 1.5 lower than that required to generate HO-1 (or C123), or about a factor of 2.3 lower than that required for C122.

As in the tholeiitic lavas, the range in the degrees of partial melting in the Honomanu alkalic basalts may be estimated by adjusting the mafic lavas for olivine fractionation. After correction for olivine fractionation, the four mafic alkalic lavas (MgO > 7%) have very similar abundances in highly incompatible elements (Fig. 12c). For example, the fractionation-corrected alkalic lavas have abundances of incompatible elements which vary by only a factor of 1.1 (Nb, La, Ce) to 1.2 (Ba, Sr); therefore, the degrees of partial melting for the Honomanu alkalic basalts varied by less than a factor of 1.2.

In summary, if sample C122 is derived by ~15% melting (Chen and Frey 1985), the Honomanu tholeiitic lavas reflect a melting range of ~10 to 15%, and the intercalated Honomanu alkalic basalts reflect a range of ~6.5 to 8% melting.

Constraints on mineralogy of the sources and residues

The isotopic similarity of the alkalic and tholeiitic Honomanu lavas combined with the higher incompatible element abundances in the alkalic lavas implies that these magmas were derived from the same source composition, but the alkalic basalts were derived by lower degrees of melting. Although the mafic (7% to 19% MgO) alkalic and tholeiitic lavas define similar trends in most major and compatible element plots (Figs. 4–6), comparisons of lavas with ~9 to 11% MgO show that the alkalic basalts have lower Sc contents than the tholeiitic basalts (Fig. 6a). Lower Sc contents in lavas that were derived by lower degrees of melting requires that the bulk residual solid/melt partition coefficient for Sc was >1. Consequently, a residue with abundant clinopyroxene (33% for $D^{cpx/l} \sim 3$) or significant garnet (25% for $D^{gt/l} \sim 4$) is required. The higher La/Sm, La/Eu, and La/Yb ratios in the alkalic basalts compared to the tholeiites (Fig. 9e–f) is consistent with the inference that clinopyroxene and garnet are in the residual mantle. Moreover, the mafic alkalic basalts and tholeiites have very similar HREE (Yb and Lu) abundances (e.g., Yb = 2.1 to 2.3 ppm for alkalic basalts and 2.2 to 2.3 for tholeiites with MgO ~8 to 9%; Table 1; Yb = 1.6 to 1.8 for fractionation-corrected mafic tholeiitic and alkalic basalts) which indicate that the bulk partition coefficients for HREE between the solid and the liquids were very close to 1. Because clinopyroxene/basaltic melt partition coefficients are <1 for REE (Green and Pearson 1985), the Sc and REE data require that garnet was residual during the partial melting processes that formed the Honomanu primary magmas.

In MgO variation plots abundances of the compatible trace elements, Cr, Co, and Ni, in the alkalic and tholeiitic Honomanu lavas define the same trends (e.g., Fig. 6c–d). Although these magma types were derived by different degrees of melting, the primary tholeiitic and alkalic lavas had similar Cr, Co and Ni abundances. This result requires residual solid/melt partition coefficients for Cr, Co and Ni that were >1. A residue containing olivine and/or orthopyroxene is implied.

As discussed earlier the abundance ratios, Nb/La, La/Ce, La/Sr, Hf/Sm, Zr/Hf and Ti/Eu are similar in the alkalic and tholeiitic Honomanu lavas. The constancy of these ratios is consistent with a compositionally homogeneous source for the Honomanu alkalic and tholeiitic basalts, and a residual peridotite mineralogy. However, a surprising result is that the alkalic basalts consistently have higher Ba/La ratios than the tholeiites (Figs. 8d and 9a). Because the tholeiites were generated by larger degrees of partial melting than the alkalic basalts, lower Ba/La ratios in the tholeities (8.3 ± 1.7) than the alkalic basalts (10.5 ± 1.4) imply that Ba was significantly more incompatible than La.

Among the major minerals of a peridotite assemblage, clinopyroxene is the most likely phase to control Ba/La in an equilibrium melt. The capacity of residual clinopyroxene to control Ba/La is shown in Fig. 13. For degrees of melting >3%, the ~25% observed Ba/La variation requires a large amount, >33%, of residual clinopyroxene for average reported partition coefficients ($D^{cpx/l} = 0.05$ for La, $D^{cpx/l} = 0.003$ for Ba; Philpotts and Schnetzler 1970; Hart and Brooks 1974; Arth 1976). Alternatively, the Ba/La differences may reflect larger cpx/melt partition coefficients. Other minerals such as plagioclase, amphibole, biotite, and phlogopite are also capable of fractionating Ba from La during basalt petrogenesis. However, Ba is more compatible than La in these mineral (Philpotts and Schnetzler 1970; Hart and Brooks 1974; Arth 1976). If plagioclase, amphibole, biotite, or phlogopite were present in the mantle residue, the alkalic basalts (derived by smaller degrees of partial melting) should have lower Ba/La ratio than the tholeiitic lavas which is opposite to the observed trend (Figs. 8d and 9a).

We conclude that the alkalic and tholeiitic Honomanu lavas may have been derived from compositionally similar sources and that the residual mineralogy contained olivine/orthopyroxene plus significant amounts of clinopyroxene and garnet. Although this residual mineralogy is similar to that inferred from other trace element studies of Hawaiian lavas (Budahn and Schmitt 1985; Feigenson et al. 1983; Hofmann et al. 1984), it contrasts markedly with interferences based on experimental melting studies. For example, Falloon et al. (1988) conclude that Hawaiian tholeiites equilibrated with harzburgite (clinopyroxene and garnet absent) residues if they were generated by anhydrous partial melting of pyrolite at less than 30 kb pressure. However, garnet

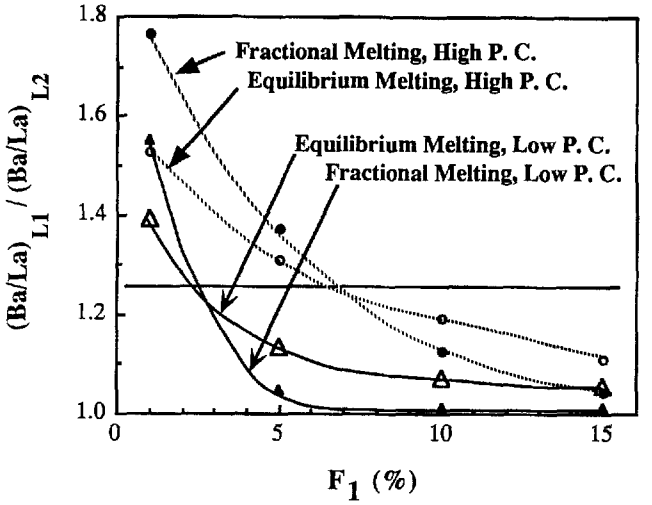

Fig. 13a, b. Variation of (Ba/La) ratio between two liquids (L_1 and L_2) as a function of F_1 (degree of partial melting which generated L_1) for the case where F_2 equals 2 times F_1. Calculated results are shown for batch melts and aggregated fractional melts. The *solid horizontal line* at Ba/La = 1.26 indicates the average difference between the alkalic and tholeiitic lavas of the Honomanu Basalt. The two cases show the effects of different partition coefficients: **a** *solid lines* represent the case where the bulk partition coefficients for Ba and La are assumed to be 0.001 and 0.0167. If average clinopyroxene/basaltic melt partition coefficients for Ba and La are used (i.e., 0.0003 for Ba and 0.05 for La, e.g., Philpotts and Schnetzler 1970; Hart and Brooks 1974; Arth 1976), the *solid line* corresponds to a case with 33% of clinopyroxene in the residue. Compared to most mantle-derived peridotites occurring as xenoliths or massif peridotites, this is an unrealistically large amounts of residual clinopyroxene. Moreover, even with this large amount of clinopyroxene the observed Ba/La fractionation requires that F_1 be $\leq 3\%$. **b** *Dotted lines* correspond to a case with higher bulk partition coefficients, i.e., 0.003 for Ba and 0.05 for La. In this case, the observed Ba/La variation is created at $F_1 \sim 7\%$

is a stable solidus phase at pressure >30 kb for anhydrous partial melting, or >20 kb in the presence of small (<0.3 wt %) water contents (Green 1973). Therefore, the significant role of garnet in the mantle residue inferred from trace elements abundances implies that the Hawaiian lavas are generated at >30 kb pressure for anhydrous melting, or >20 kb if the water is present.

Interpretations of the temporal geochemical trends defined by lavas from Haleakala Volcano

Because the stratigraphic section in Honomanu Gulch includes the transition from the Honomanu Basalt to the Kula Volcanics, we can integrate the geochemical trends defined by lavas in Honomanu Gulch with those in the Nahiku drill cores (Chen and Frey 1985). As shown in Fig. 8a and Table 1 the two youngest Honomanu lavas (HO-13 and HO-12) and the oldest Kula lava (HO-11) demonstrate that there is a gradational decrease in $^{87}Sr/^{86}Sr$ across the Honomanu Basalt-Kula Volcanics boundary. As shown by Chen and Frey (1983, 1985) this decrease in $^{87}Sr/^{86}Sr$ with decreasing eruption age is characteristic of the Nahiku drill cores which contain lavas from the Kula and Hana Volcanics. This temporal $^{87}Sr/^{86}Sr$ trend is accompanied by systematic variations in abundance ratios such as Nb/La, La/Ce, Sm/Nd and Rb/Sr. Chen and Frey (1983, 1985) interpreted these temporal geochemical variations as reflecting a systematic change in mixing proportions between melts derived from a plume-derived component and depleted, MORB-related mantle component, coupled with a temporal decrease in the extent of melting that created the depleted melt ("depleted" in terms of a lower Sr isotopic ratio). This depleted melt was interpreted to be derived from the oceanic lithosphere, but entrainment of MORB-related asthenosphere in an ascending plume (Griffiths 1986) is another possibility. Kurz et al. (1987) reported $^3He/^4He$ data for several samples from the Nahiku drill cores and Honomanu Gulch. The systematically higher $^3He/^4He$ in Honomanu lavas (13.1 to 16.8 Ra) and the MORB-like $^3He/^4He$ ratios in Kula and Hana lavas (6.6 to 8.3 Ra) are consistent with mixing between plume-related and depleted, MORB-related mantle components.

The models proposed by Chen and Frey (1983, 1985) used batch melting. Ribe (1988) recently evaluated a more sophisticated "dynamical model" for melting of an ascending plume. In this model melts segregated from a partially melted ascending plume have higher abundances of incompatible elements than melts derived by equivalent amounts of batch melting. Although different melting models for the plume were used by Chen and Frey (1983, 1985) and Ribe (1988), both approaches conclude that $^{87}Sr/^{86}Sr$ and incompatible element abundance ratios, such as La/Ce, in Haleakala lavas are primarily controlled by the degree of melting of the MORB-related mantle component; i.e., oceanic lithosphere in these models. Specifically, the temporal increase of La/Ce and decrease of $^{87}Sr/^{86}Sr$ defined by lavas from the Honomanu Basalt, Kula Volcanics, and Hana Volcanics requires the degree of partial melting of the lithosphere to decrease with time (Fig. 9 Chen and Frey 1985; Figs. 4–7 Ribe 1988). However, the inferred degrees of partial melting in the lithosphere depend strongly on the trace element partition coefficients utilized. For example, if the plume component is assumed to have bulk earth $^{87}Sr/^{86}Sr$ and La/Ce ratios, and bulk solid/melt partition coefficients for La and Ce are assumed to be 0.0025 and 0.005 ($D_{Ce}/D_{La} = 2$), respectively (Chen and Frey 1983, 1985), then La/Ce ratios in Honomanu lavas require ~0.5 to 2% melting of lithosphere for a batch melting model. This range of partial melting successfully accounts for La/Ce, $^{87}Sr/^{86}Sr$ and $^{143}Nd/^{144}Nd$ ratios (Fig. 9 Chen and Frey 1985). However, this choice of La and Ce partition coefficients leads to ~1 to 2% lithosphere melting in the dynamical melting model (Fig. 6, Ribe 1988), and this result is inconsistent with the inferred 5–10% melting of the lithosphere that is required to account for $^{87}Sr/^{86}Sr$ and $^{143}Nd/^{144}Nd$ in the dynamical melting model (Figs. 4 and 5, Ribe 1988). In order to eliminate this inconsistency, Ribe (1988) used lower La and higher Ce partition coefficients (i.e., $D_{La} = 0.001$ and $D_{Ce} = 0.01$), that is, a much larger D_{Ce}/D_{La} ratio (10). Although the required 5 to 10% lithosphere melting was presented as a significant difference from the results of Chen and Frey (1983, 1985), we note that with this choice of partition coefficients, 4 to 10% melting of the lithosphere is also required by the batch melting model.

Thus, the results of both models are similar for this choice of partition coefficients. Is a D_{Ce}/D_{La} ratio of 10 reasonable? With such a large difference in partition coefficients, significant variations in La/Ce should result from varying degrees of melting. Specifically, the range in degree of melting required by incompatible element abundances in Honomanu lavas, a factor of ~2.3, should result in systematically varying La/Ce ratios in Honomanu lavas. The anticipated positive correlation between La/Ce and La content (a measure of degree of melting) is not seen in the Honomanu lavas (Fig. 9c). We conclude that a D_{Ce}/D_{La} of ~2 is more likely than a value of ~10.

Finally, the uniformity of isotopic and abundance ratios involving highly incompatible elements in the Honomanu lavas requires a source homogeneity that is not observed in lavas from the Kula and Hana Volcanics. Possibly, the Honomanu lavas represent a pure plume component. However, given the isotopic diversity of lavas from different Hawaiian shields (Stille et al. 1986; West et al. 1987), the diversity of mantle components that may be represented in Hawaiian lavas (Wyllie 1988), and the possibility of plume-asthenosphere mixing during ascent (Griffiths 1986), it is more likely that these Honomanu lavas reflect a brief stage of volcano evolution when the mixing proportions of mantle components were approximately constant. In either case, the variable incompatible element contents reflected by the intercalated alkalic and tholeiitic Honomanu lavas coupled with near isotopic homogeneity are easiest to interpret as resulting from different extents of melting. For example, the center of a plume will be hotter than the margins and this should create a gradient in extent of melting. Therefore, the intercalated tholeiitic and alkalic Honomanu lavas may reflect a process which tapped melts generated in different portions of a rising plume.

Conclusions

This geochemical study of a stratigraphic section through the oldest subaerially exposed lavas on Haleakala Volcano, a 250 m section in Honomanu Gulch, complements previous geochemical studies of younger stratigraphic sections (Chen and Frey 1985; Chen et al. 1990; West and Leeman 1987). Major results and conclusions are:

A. This section of the Honomanu Basalt contains intercalated tholeiitic and alkalic lavas ranging in age from ~1.1 to 0.97 Ma. There is a continuous gradation from tholeiitic to alkalic compositions. Because only alkaline lavas occur in the overlying Kula and Hana Volcanics, this section of the Honomanu Basalt represents a transition from tholeiitic to alkalic volcanism.

B. Samples from the lower 200 m of section are marginally heterogeneous in Sr, Nd and Pb isotopic ratios (e.g., $^{87}Sr/^{86}Sr$ ranges from 0.70371 to 0.70384 for 15 samples), but there are no systematic temporal variations in these isotopic ratios. Moreover, there is complete isotopic overlap between the tholeiitic and alkalic lavas. Abundance ratios involving elements of similar incompatibility, such as Nb/La, La/Ce, La/Sr, Nb/La, Hf/Sm, Zr/Hf, Ti/Eu, are also similar in these alkalic and tholeiitic Honomanu lavas. These isotopic and incompatible element abundance data are consistent with derivation of the alkalic and tholeiitic Honomanu lavas from compositionally similar mantle sources.

C. The MgO-rich Honomanu lavas establish that a range of tholeiitic parental magma compositions were erupted; perhaps representing primary magmas formed over a small range in degree of melting. One of the tholeiitic lavas in this Honomanu section is similar in major element composition to submarine lavas dredged from the east rift of Haleakala (Moore et al. 1990), but all other tholeiitic lavas in Honomanu Gulch are compositionally distinct from these submarine glasses.

By assuming the same source composition for alkalic and tholeiitic lavas, we infer that the tholeiitic lavas formed over a range in degree of melting (a factor of ~1.5, e.g., 10% to 15% melting), and that the alkalic lavas formed by a lower degree of melting (~a factor of 1.5 lower than the tholeiitic lavas, e.g., 6.5 to 8% if the tholeiitic lavas formed by 10 to 15% melting).

After a first-order correction for post-melting crystal-melt fractionation (i.e., olivine, addition to lavas with >7% MgO), the calculated tholeiitic and alkalic parental magmas have very similar compatible trace element and heavy REE contents, but the alkaline lavas have lower Sc contents and higher Ba/La. If the same source composition is assumed for these Honomanu lavas, a peridotite residue containing significant amounts of clinopyroxene and garnet is required.

D. The uppermost Honomanu lavas (~0.97 Ma) in this section and three overlying Kula lavas (~0.78 to 0.93 Ma) establish that during this time period $^{87}Sr/^{86}Sr$ gradually decreases, from 0.70371 to 0.70328. This result is consistent with the previously defined temporal changes in $^{87}Sr/^{86}Sr$ during eruptions of the Kula Volcanics (Chen and Frey 1985; West and Leeman 1987). These isotopic and accompanying trace element abundance changes require a mixing model, and the geochemical trends are consistent with mixing between components derived from a plume-related source and a depleted MORB-related source. Apparently, during the waning stages of volcanism (~0.97 Ma to present) there has been a systematic change in mixing proportions with an increasing contribution from the MORB-related component.

Acknowledgement. We thank D.A. Clague, M. Lanphere, T.L. Wright and the Geologic Names Unit of U.S. Geological Survey for thorough and constructive reviews of the paper. We also thank J.M. Rhodes for access to XRF facilities, Jerzy Blusztajn for obtaining Sr and Nd isotopic data for sample HO-21, S. Rowland for assistance with the fluxgate magnetometer measurements and J. Knox for finishing touches to the figures. Neutron irradiations were made at the MIT Nuclear Reactor. This research was supported by Research Board, University of Illinois and NSF (EAR 8705809 to FAF; OCE8716042 to MOG). Hawaii Institute of Geophysics contribution no. 2350.

References

Arth JG (1976) The behavior of trace elements during magmatic processes: a summary of theoretical models and their applications. J Res US Geol Survey 4:41–47

Berggren WA, Kent DV, van Couvering JA (1985) Neogene geochronology and chronostratigraphy in the chronology of the geological record. Geol Soc London Mem 10:211–260
Budahn JR, Schmitt RA (1985) Petrogenetic modeling of Hawaiian tholeiitic basalts: a geochemical approach. Geochim Cosmochim Acta 49:67–87
Chen C-Y (1987) Lead isotopic constraints on the origin of Hawaiian basalts. Nature 327:49–52
Chen C-Y (1990) High magnesium primary magmas from Haleakala Volcano, Hawaii. Trans Am Geophys Eos 71:968
Chen C-Y, Frey FA (1983) Origin of Hawaiian tholeiite and alkalic basalt. Nature 302:785–789
Chen C-Y, Frey FA (1985) Trace element and isotopic geochemistry of lavas from Haleakala volcano, East Maui, Hawaii: implications for the origin of Hawaiian basalts. J Geophys Res 90:8743–8768
Chen C-Y, Frey FA, Garcia MO (1990) Evolution of alkalic lavas at Haleakala Volcano, east Maui, Hawaii: major, trace element and isotopic constraints. Contrib Mineral Petrol (in press)
Clague DA, Dalrymple GB (1987) The Hawaiian-Emperor volcanic chain. Part 1. Geologic evolution. USGS Prof Pap 1350:5–54
Dalrymple GB, Lanphere MA (1969) Potassium-argon dating. Freeman, San Francisco, 258 pp
Doell RR, Dalrymple GB (1973) Potassium-argon ages and paleomagnetism of the Waianae and Koolau Volcanic Series, Oahu, Hawaii. Geol Soc Amer Bull 84:1217–1242
Falloon TJ, Green DH, Hatton CJ, Harris KL (1988) Anhydrous partial melting of a fertile and depleted peridotite from 2 to 30 kb and application to basalt petrogenesis. J Petrol 29:1259–1282
Feigenson MD, Spera FJ (1981) Dynamical model for temporal variation in magma type and eruption interval at Kohala Volcano, Hawaii. Geology 9:531–533
Feigenson MD, Hofmann AW, Spera FJ (1983) Case studies on the origin of basalt. II. The transition from tholeiitic to alkalic volcanism on Kohala volcano, Hawaii. Contrib Mineral Petrol 84:390–405
Frey FA, Wise WS, Garcia MO, West H, Kwon ST, Kennedy A (1990) Evolution of Mauna Kea Volcano, Hawaii: the transition from shield building to the alkalic cap stage. J Geophys Res 95:1271–1300
Green DH (1973) Experimental melting studies on a model upper mantle composition at high pressures under water-saturated and water-undersaturated conditions. Earth Planet Sci Lett 19:37–53
Green TH, Pearson NJ (1985) Rare earth element partitioning between clinopyroxene and silicate liquid at moderate to high pressure. Contrib Mineral Petrol 91:24–36
Griffiths RW (1986) The differing effects of compositional and thermal buoyancies on the evolution of mantle diapirs. Phy Earth Planet Inter 43:261–273
Hart SR, Brooks C (1974) Clinopyroxene-matrix partitioning of K, Rb, Cs, Sr and Ba. Geochim Cosmochim Acta 38:1799–1806
Hofmann AW, Feigenson MD, Raczek I (1984) Case studies on the origin of basalt. III. Petrogenesis of the Mauna Ulu eruption, Kilauea, 1969–1971. Contrib Mineral Petrol 88:24–35
Ingamells CO (1970) Lithium metamorage flux in silicate analysis. Analy Chim Acta 52:332–334
Kurz MD, Garcia MO, Frey FA, O'Brien PA (1987) Temporal helium isotopic variation within Hawaiian volcanoes: basalts from Mauna Loa and Haleakala. Geochim Cosmochim Acta 51:2905–2914
Langenheim VAM, Clague DA (1987) The Hawaiian-Emperor volcanic chain. Part II. Stratigraphic framework of volcanic rocks of the Hawaiian island. US Geol Survey Prof Pap 1350:55–84
Lockwood JP, Lipman PW (1987) Holocene eruptive history of Mauna Loa Volcano. US Geol Surv Prof Pap 1350:509–535
Maaloe S, Hansen B (1982) Olivine phenocrysts of Hawaiian olivine tholeiite and oceanite. Contrib Mineral Petrol 81:203–211
Macdonald GA, Katsura T (1964) Chemical composition of Hawaiian lavas. J Petrol 5:82–133
Macdonald GA, Abbott AT, Peterson FL (1983) Volcanoes in the sea: the geology of Hawaii, 2nd edn. University of Hawaii Press, Honolulu
McDougall I (1964) Potassium-argon ages from lavas of the Hawaiian Islands. Bull Geol Soc Am 75:107–128
Moore JG, Campbell JF (1987) Age of tilted reefs, Hawaii. J Geophys Res 92:2641–2646
Moore JG, Fiske RS (1969) Volcanic substructure inferred from dredge samples and ocean-bottom photographs, Hawaii. Geol Soc Am Bull 80:1191–1201
Moore JG, Clague DA, Ludwig KR, Mark RK (1990) Subsidence and volcanism of the Haleakala Ridge, Hawaii. Volcanology and Geothermal Res (in press)
Naughton JJ, Macdonald GA, Greenberg VA (1980) Some additional potassium-argon ages of Hawaiian rocks: The Maui Volcanic Complex of Molokai, Maui, Lanai and Kahoolawe. J Volcanol Geotherm Res 7:339–355
Philpotts JA, Schnetzler CC, Thomas HH (1972) Petrogenetic implications of some new geochemical data on ecologite and ultrabasic inclusions. Geochim Cosmochim Acta 36:1131–1166
Ribe NM (1988) Dynamical geochemistry of the Hawaiian plume. Earth Planet Sci 88:37–46
Spengler SR, Garcia MO (1988) Geochemistry of Hawi lavas, Kohala Volcano, Hawaii. Contrib Mineral Petrol 99:90–104
Stacey JS, Sherrill ND, Dalrymple GB, Lanphere MA, Carpenter NV (1981) A five collector system for the simultaneous measurement of argon isotope ratios in a static mass spectrometer. Int Mass Spectrom Ion Phys 39:167–180
Stearns HT, Macdonald GA (1942) Geology and groundwater resources of the Island of Maui, Hawaii. Hawaii Div Hydrograph Bull 7:344 pp
Steiger RH, Jager E (1977) Subcommission on geochronology: Convention on the use of decay constants in geo- and cosmochronology. Earth Planet Sci Lett 36:359–362
Stille P, Unruh DM, Tatsumoto M (1986) Pb, Sr, Nd and Hf isotopic constraints on the origin of Hawaiian basalts and evidence for a unique mantle source. Geochim Cosmochim Acta 50:2303–2319
Sun S-S, McDonough WF (1989) Geochemical and isotopic systematics of oceanic basalts: implications for mantle composition and processes. Geol Soc Special Pub 42:313–345
Taylor JR (1982) An introduction to error analysis. University Science Books, Mill Valley, 270 pp
West HB, Leeman WP (1987) Isotopic evolution of lavas from Haleakala Crater, Hawaii. Earth Planet Sci 84:211–225
West HB, Gerlach DC, Leeman WP, Garcia MO (1987) Isotopic constraints on the origin of Hawaiian lavas from the Maui Volcanic Complex, Hawaii. Nature 330:216–219
Wilde P, Chase TE, Normark WR, Thomas JA, Young JD (1980) Occanographic data off the southern Hawaiian Islands. Lawrence Berkely La Pub 359
Wright TL (1971) Chemistry of Kilauea and Mauna Loa lavas in space and time. US Geol Surv Prof Pap 735:40 pp
Wyllie PJ (1988) Solidus curves, mantle plumes, and magma generation beneath Hawaii. J Geophys Res 93:4171–4181

Editorial responsibility: T. Grove